CHAPTER I

INTRODUCTION

Description of the Cerebellum

Over a century ago, the neuronal circuitry of the cerebellum was reported by Santiago Ramon y Cajal (1888), he described five neurons that comprise the cerebellar cortex. These neurons are arranged within three distinct layers to form a circuit, thus enabling the cerebellum to receive extracortical synaptic information. After processing incoming information it channels signals toward deep cerebellar nuclei, vestibular nuclei and brainstem nuclei (De Camilli et al., 1984). The deepest or most ventral of these layers is comprised of excitatory granule neurons, the most abundant neuron throughout the entire brain. These neurons form synapses and receive excitatory inputs from afferent mossy fibers, which project into the cerebellum from other areas of the central nervous system (CNS). The granule neuron has a single projection extending dorsally into the most superficial layer, the molecular layer. This single projection then bifurcates to form parallel fibers extending as far as 3 mm in each direction from its point of branching. Within the molecular layer the parallel fibers form synapses with excitatory climbing fibers and inhibitory basket cells, stellate cells, golgi cells and the expansive dendritic arbors of Purkinje neurons (PNs). The cell bodies of PNs comprise the last of the three layers, the Purkinje layer, which position themselves as a single monolayer separating the granule and molecular layers.

The PN has characteristic morphological features that distinguish it from other cell types. The dendritic tree of a PN has the most extensive branching pattern of any neuron. It also serves as the only efferent neuron in the cerebellum by sending a single axonal projection ventrally to deep cerebellar nuclei. Depending on the region of the cerebellum where the PN is located, it projects to corresponding cerebellar nuclei, which relay signals to various output peduncles that synapse with midbrain structures (thalamus, red nuclei and premotorcortex), dorsal brainstem or cerebral neocortex (de Zeeuw and Berrebi, 1996). A schematic depicting these cell types and their circuitry is shown in Figure 1.1.

All of these neurons are thought to arise from two separate zones of cell division, the ventricular zone and the rhombic lip (Figure 1.2). The mechanisms controlling the proliferation and migration of granule neurons within the rhombic lip have been extensively characterized (Alder et al., 1999; Goldowitz and Hamre, 1998; Lin and Cepko, 1998; Wingate, 2001; Wingate and Hatten, 1999). For example, guidance cues such as Netrin1 and Slit2 guide anterior migration to form the external granule layer located at the most dorsal region of the cerebellum, which then receives cues such as a secreted Hedghog (Hh) protein, signaling granule neurons to begin proliferation and start their ventral migration to form the granule layer (Alder et al., 1996; Dahmane and Ruiz i Altaba, 1999; Gilthorpe et al., 2002; Goodrich et al., 1997; Hager et al., 1995; Hatten and Heintz, 1995; Koster and Fraser, 2001; Wechsler-Reya and Scott, 1999). By contrast, the mechanisms that regulate migration, proliferation and organization of the other cerebellar cell types are poorly understood.
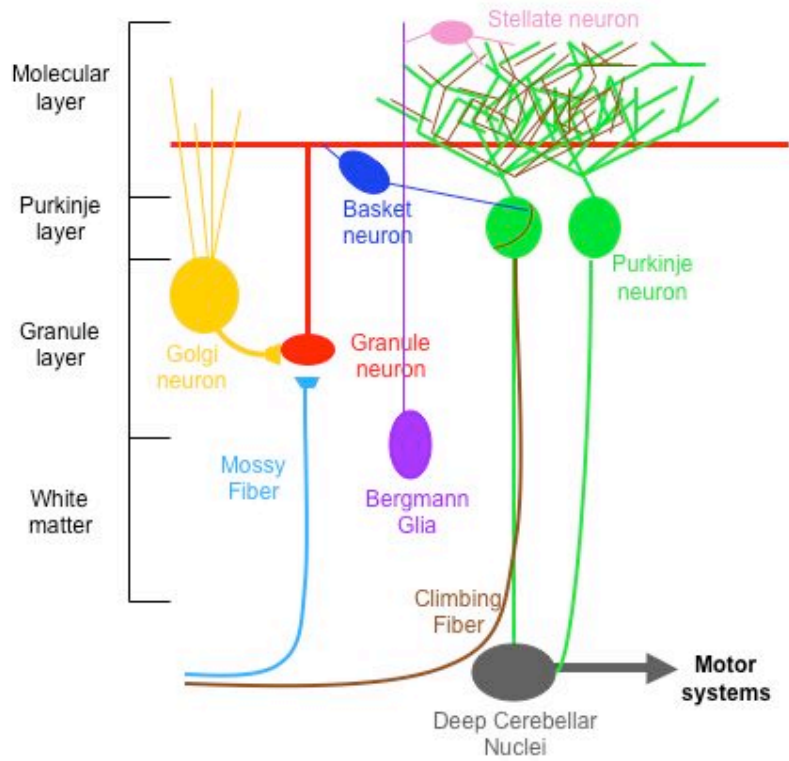
Figure 1.1. *Schematic diagram depicting the neuronal circuitry in a mammalian cerebellum.*
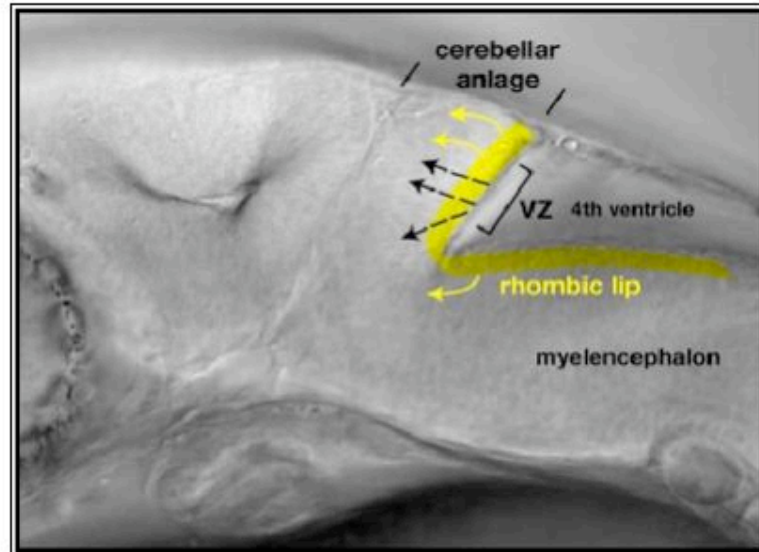
Figure 1.2. *All cerebellar neurons arise from either the rhombic lip or the ventricular zone.* 24 hpf embryo with anterior left, dorsal to the top. Yellow highlighted region depicts rhombic lip where granule neurons and deep cerebellar nuclei undergo anterior and ventral migration. Bracketed region depicts the ventricular zone where all other cerebellar cell types are thought to arise.

Signaling Pathways that Pattern

Throughout all of animal development, in both invertebrate and vertebrate systems, certain signaling pathways have repeatedly been demonstrated to regulate aspects such as proliferation, migration and patterning. These signaling pathways often interact with each other and are usually required to be in the presence of one another to allow for proper embryonic development. Three of these pathways, Bone Morphogenetic Proteins (BMPs), Wnt signaling and Hh singaling have well established roles for many aspects of development including patterning the dorsoventral (DV) axis of the spinal cord. The roles these signals play in patterning the spinal cord provide clues that may give us insight into their potential roles in patterning the DV axis of the cerebellum.

Hedgehog Signaling

The Hh protein was identified in a genetic screen in *Drosophila melanogaster* to find mutations that disrupt body patterning (Nusslein-Volhard and Wieschaus, 1980). There are three vertebrate homologs of Hh in mammalian systems, Sonic hedgehog (Shh), Indian hedgehog (Ihh) and Desert hedgehog (Dhh). However, the mechanics of how the pathway works are generally conserved from flies to human. In mammals, all Hhs are secreted proteins, however, before they can be secreted they undergo autocatalytic cleavage by their carboxy-terminus, leaving the 19 kDa signaling amino-terminus. Cholesterol modification of the carboxy-terminus and palmitolation of the amino-terminus of this 19 kDa peptide is usually an additional step before the active Hh signal can

be transported and released at the cell surface by the twelve-transmembrane G protein coupled receptor, Dispatched (Disp) (Beachy et al., 1997; Cooper et al., 1998; Ingham and McMahon, 2001; Mann and Beachy, 2004; Taipale and Beachy, 2001). Once secreted, the Hh protein can have both short and long range signaling. Cells expressing the twelve-membrane G protein coupled receptor, Patched (Ptc), at their surface are then able to receive the Hh ligand. When no Hh protein is present, a complex involving Costal 2 (Cos2), Suppressor of Fused (SuFu) and Iguana allows a repressor form of the protein Gli (Gli^R) to be translocated into the nucleus, blocking any transcription of downstream targets of the Hh pathway. Once the Hh protein binds to Ptc, it begins a signaling cascade starting with the release of the seven-transmembrane protein Smoothened (Smo). Smo is normally inhibited by Ptc in the absence of the Hh protein, although the mechanism for this remains unclear (Taipale et al., 2002). Smo then acts on the SuFu complex to block activation of the Gli^R and instead an activated Gli (Gli^A) is translocated into the nucleus, activating downstream targets of the Hh pathway (Figure 1.3).

Bone Morphogenetic Proteins

BMPs are growth factors that belong to the transforming growth factor ß (TGFß) superfamily. BMP activity was first reported in a study involving bone formation (Kingsley, 1994; Urist, 1965), and has since been described as a critical protein during multiple aspects of embryonic development such as DV and anterior-posterior (AP) axis formation, epidermal induction, neural crest

6

Figure 1.3. *Schematic diagram of Hh pathway.* (A) The cell secreting the Hh ligand, illustrating the cholesterol modification and palmitolation that occurs before the ligand is secreted through the receptor Disp. (B) This schematic represents the inner portion of the cell in the absence of the Hh ligand. Repression of Smo by Ptc results in Gli^R translocating into the nucleus, preventing activation of downstream targets of the Hh pathway. (C) The schematic on the right represents a cell in the presence of a Hh ligand in which inhibition of Smo is released, resulting in activation of downstream targets of the Hh pathway.
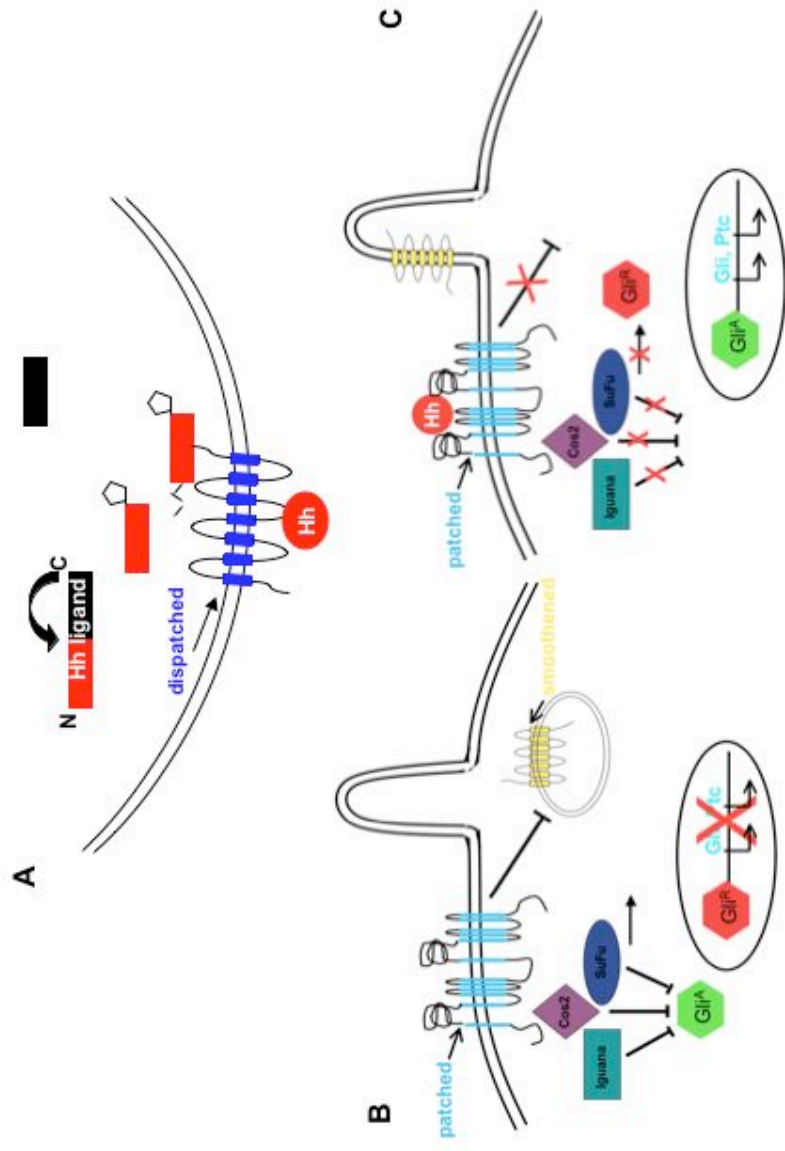
development and limb bud formation (Chen et al., 2004; Christiansen et al., 2000; Munoz-Sanjuan and Brivanlou, 2002; Niswander and Martin, 1993; Wall and Hogan, 1994). Mutations in *decapentaplegic* (*dpp*), the *Drosophila* homologue of mammalian BMP-2 and BMP-4, cause DV patterning defects very early in development (Nakayama et al., 2000; Ray et al., 1991). Much like the Hh protein, BMPs are secreted and can transmit both short and long range signaling. There are numerous types of BMPs, but all undergo some form of proteolytic cleavage event within the secretory pathway and bind to a receptor complex composed of dimers of type I and type II transmembrane serine/threonine kinases (Constam and Robertson, 1999; Wrana et al., 1994). Upon ligand binding, type II receptors phosphorylate the GS box in type I receptors, activating their kinase activity (Yamashita et al., 1996), which then allows the type I receptors to phosphorylate downstream targets of the pathway. Transduction of the BMP pathway is dependant on phosphorylation of Smads. There are three families of Smads, common Smads (Co-Smads), receptor-regulated Smads (R-Smads) and inhibitory Smads (Anti-Smads) (Kawabata and Miyazono, 1999; Whitman, 1998). Once the type I receptor is phosphorylated, it can then phosphorylate R-Smads (Smad 1/5/8) which causes a conformational change that leads to dissociation of the R-Smad from the type I receptor, allowing interaction with a Co-Smad (Smad 4). This results in a complex that is then translocated into the nucleus and functions to regulate transcription of target genes (Christian and Nakayama, 1999; Zhang and Derynck, 1999). In addition, the pathway can also be controlled by Anti-Smads (Smad 6/7) binding to the type

I receptor after the BMP ligand has joined the type I/type II receptor complex (Imamura et al., 1997). Inactivation of the pathway can also occur before the BMP ligand is present through degradation of the R-Smads by Smurf1, an E3 ubiquitin ligase (Figure 1.4) (Zhu et al., 1999).

The Wnt Pathway

Wnt proteins were first identified in flies from mutations of *wingless* (*wg*), a segment polarity gene found in the same screen Hh was identified (Nüsslein-Volhard and Wieschaus, 1980). The Wnt signaling pathway is highly conserved from invertebrate to vertebrate systems and has multiple roles in cell fate specification, DV patterning, differentiation and mitogenic stimulation. In the absence of Wnt ligand, a cytosolic complex involving Axin, Adenomatous Polyposis Coli (APC), glycogen synthase kinase- 3ß (GSK-3) and ß-catenin results in phosphorylation of ß-catenin by serine/threonine kinases, thus allowing for its intracellular degradation (Amit et al., 2002; Liu et al., 2002). Involvement of ß-catenin in the Wnt pathway is termed the canonical pathway, without involvement of ß-catenin, the pathway is called the non-canonical pathway (Logan and Nusse, 2004). The canonical pathway is most commonly known for roles in patterning and axis formation, the non-canonical pathway is usually involved in cell polarization (Strutt, 2003). Similar to Hh and BMPs, Wnt ligands are able to have both short and long range signaling effects and undergo modification prior to secretion. A highly conserved cysteine residue within the

Figure 1.4. *Schematic diagram of BMP pathway.* (A) The cell secreting the BMP ligand, illustrating the proteolytic cleavage event that occurs before the ligand is secreted. (B) This schematic represents the cytoplasmic portion of the cell in the absence of the BMP ligand. R-Smad's interact with SMURFs, preventing them from being phosphorylated and being in the nucleus, thus preventing activation of downstream targets of the BMP pathway. (C) This schematic shows that in the presence of the BMP ligand the Type I and Type II receptors bind the ligand, causing a phosphorylation event which in turn causes R-Smads and Co-Smads to interact and activate downstream targets of the BMP pathway.
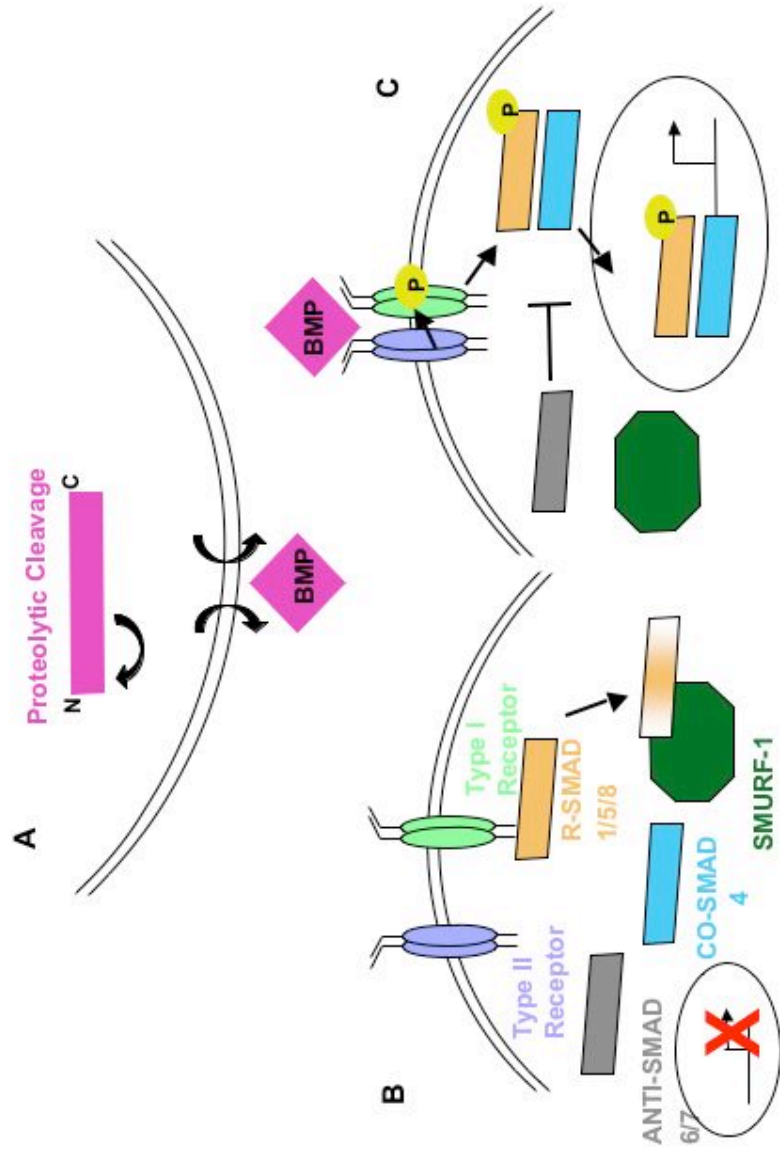
Wnt protein is palmitolated, subsequently giving rise to its active form (Willert et al., 2003). Once secreted, the ligand can bind to its seven transmembrane primary receptor, Frizzled (Fz) (Bhanot et al., 1996). Activation of the Wnt pathway however, requires recruitment of its second single pass lipoprotein receptor-related protein, LRP5/6 (Pinson et al., 2000; Tamai et al., 2000). Upon binding to the Wnt ligand, the LRP receptor becomes phosphorylated allowing for interaction with the cytosolic protein Axin with Dishevelled (Dsh), a cytoplasmic protein bound to Fz (Lee et al., 1999; Tolwinski et al., 2003). This allows for Axin to become disassociated with the complex, resulting in no phosphorylation of ß-catenin, allowing it to accumulate in the nucleus (Miller and Moon, 1997; Tolwinski and Wieschaus, 2004). Once in the nucleus, ß-catenin interacts with TCF/LEF complex to activate downstream transcription regulators of the pathway (Figure 1.5) (Behrens et al., 1996; van de Wetering et al., 1997).

All three of these pathways have critical roles during embryonic development, often interacting with each other. The developing spinal cord is one example that has been well described, in which the orchestration of all three pathways is important for patterning and specification of cell types along the DV axis.

A Model for Dorsoventral Patterning

During spinal cord development, specific classes of neurons differentiate at distinct positions along the DV axis. Opposing signaling gradients from the notochord, mesodermal cells located just ventral to the forming spinal cord, and

Figure 1.5. *Schematic diagram of Wnt pathway.* (A) Before the Wnt ligand can be secreted, a highly conserved cysteine residue within the Wnt protein is palmitolated. (B) In the absence of the Wnt ligand a complex with Axin, APC, GSK-3ß and ß-catenin is phosphorylated, eventually leading to degradation of ß-catenin, preventing activation of downstream targets of the pathway. (C) Upon binding of the Wnt ligand to the Fz receptor, LRP5/6 is recruited and phosphorylated, preventing the degradation of ß-catenin which in turn activates downstream targets of the Wnt pathway.
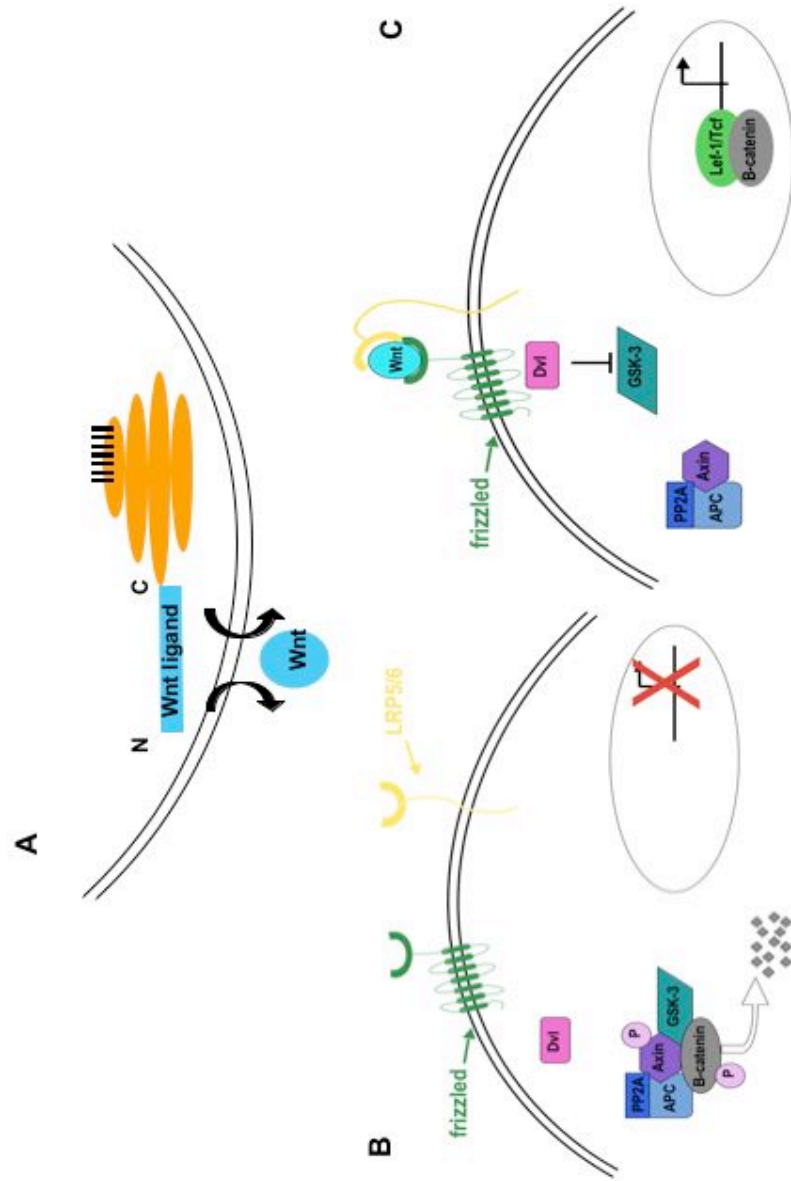
the roof plate, specialized dorsal neural tube midline cells, have been implicated as the organization centers that specify cell types in the developing spinal cord (Altman and Bayer, 1984; Dickinson et al., 1995; Liem et al., 1995; van Straaten and Hekking, 1991; van Straaten et al., 1985; Yamada et al., 1991). Signals from these organization centers, set in opposition to each other form gradients, which have been shown to antagonize each other and restrict their range of activity (Altman and Bayer, 1984; Jessell, 2000; Lee and Jessell, 1999; Liem et al., 1995; Schoenwolf, 1982). Hh is secreted from the notochord and induces formation of the floor plate. Subsequently, the notochord and floor plate serve as ventral organizing centers and generate a ventral-dorsal activity gradient of Hh signaling that promotes specification of various ventral cell types (Briscoe and Ericson, 2001; Echelard et al., 1993; Ericson et al., 1997; Krauss et al., 1993; Marti et al., 1995; Poh et al., 2002; Riddle et al., 1993; Tanabe and Jessell, 1996).

Directly adjacent to the floor plate is the p3 domain whereas just dorsal to the p3 domain is the pMN domain, both giving rise to motor neurons and ventral interneurons. The p2, p1 and p0 domains are located dorsal to the pMN domain and give rise to multiple neurons (Figure 1.6). Loss of Hh signaling in spinal cord development results in a loss or reduction of ventral neurons and an increase in dorsally located cell types as well as a dorsal to ventral expansion of dorsally secreted signals (Figure 1.7)(Aruga et al., 2002; Briscoe et al., 1999; Chiang et al., 1996; Ericson et al., 1995; Lee and Jessell, 1999; Park et al., 2004).

The roof plate, made of specialized dorsal neural tube midline cells, is the dorsal organizing center for the spinal cord. The roof plate, in most vertebrate
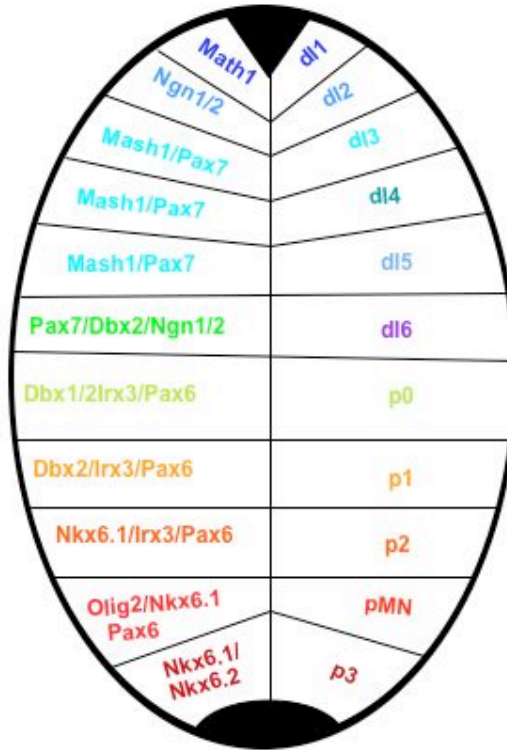
16

Figure 1.6. *A schematic representing progenitor domains and corresponding transcription factors expressed within each domain along the entire DV axis of the spinal cord.*
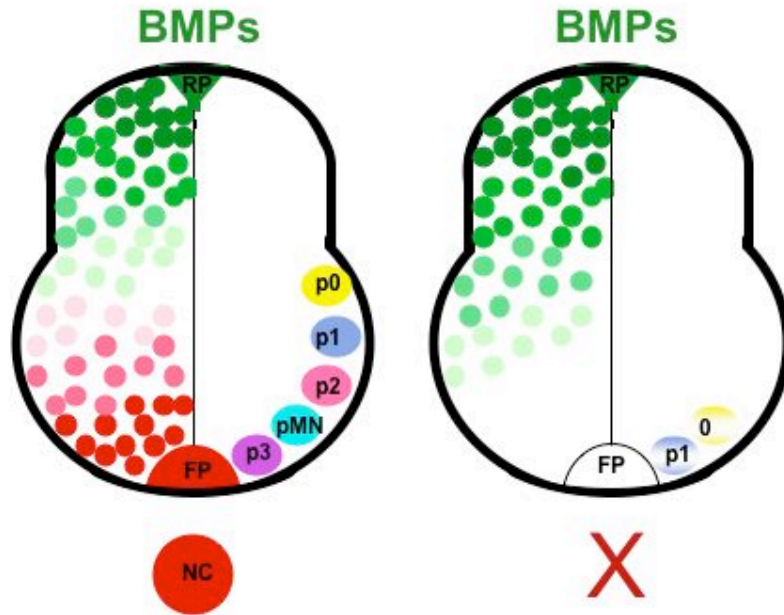
17

Figure 1.7. *Schematic for ventral specification along DV axis of spinal cord.* Figure on left represents the domains of specification which normally occur in the presence of the dorsal BMP gradient and the ventral Shh gradient. The figure on the right represents what occurs to the ventrally located domains in the absence on the Hh signaling gradient. The neurons and cell types that arise from the three ventral domains closest to the floor plate are ablated accompanied by a decrease in the number of cells that arise from the p1 and p0 domains as well as their ventral shift in position.

systems, expresses *Bmp4*, *Bmp5* and *Bmp7* and establishes a dorsal-ventral activity gradient necessary for specification of dorsal cell types (Liem et al., 1997; Liem et al., 1995). Directly adjacent to the roof plate are dl1 neurons followed by a stepwise ventral organization of dl2, dl3, dl4, dl5 and dl6 respectively (Figure 1.6). These domains give rise to multiple cell types and correspond to specific transcription factors that identify each domain. In vitro studies in chick and quail have shown that ectopic placement of roof plate can induce formation of dl1 and dl2 dorsal interneurons (Liem et al., 1997). Conversely, ablation of the roof plate results in a complete loss of dorsally located dl1 and dl2 interneurons, or a dorsal shift of more ventrally located cell types, (Lee et al., 2000; Liem et al., 1995) as well as causing an expansion of ventrally located neurons (Figure 1.8) (Lee et al., 2000). In the canonical model for DV patterning within the spinal cord, BMPs are the primary signal secreted from the roof plate necessary for patterning the dorsal half of the spinal cord. However, additional experiments revealed dorsally derived Wnt signals are important for patterning the dorsal half of the spinal cord as well (Muroyama et al., 2002; Wine-Lee et al., 2004).

As the mouse neural tube closes, *Wnt1* and *Wnt3a* are expressed in the roof plate (Parr et al., 1993). Mutations of these genes individually showed no disruption of dorsal patterning, however, embryos deficient in both *Wnt1* and *Wnt3a* show a loss of dorsally located dl1 and dl2 interneurons (McMahon and Bradley, 1990; Muroyama et al., 2002; Thomas and Capecchi, 1990). This is accompanied by an increase in ventrally located neurons, much like in the absence of BMP signals (Muroyama et al., 2002).
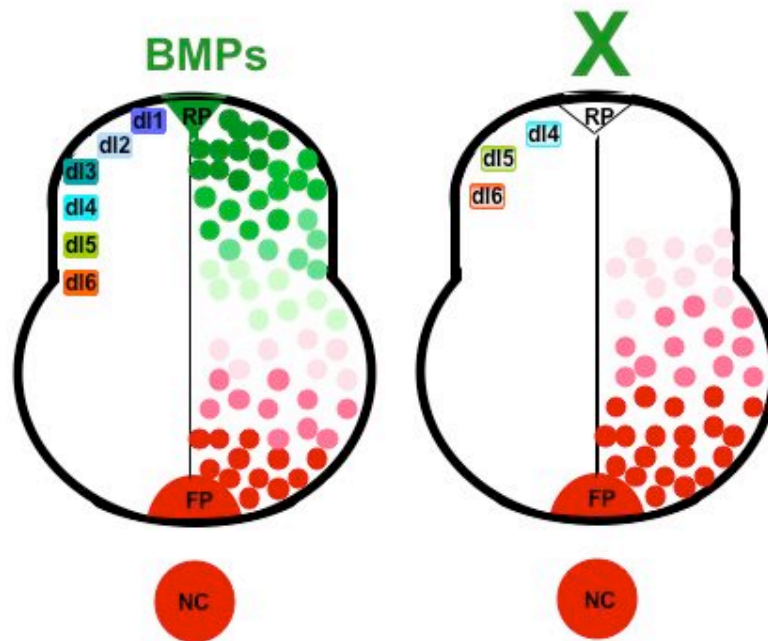
Figure 1.8. *Schematic for dorsal specification along DV axis of spinal cord.* Figure on left represents the domains of specification which normally occur in the presence of the dorsal BMP gradient and the ventral Shh gradient. The figure on the right represents what occurs to the dorsally located domains in the absence on the BMP signaling gradient. The neurons and cell types that arise from the three dorsal domains closest to the roof plate are ablated accompanied by a decrease in the number of cells that arise from the dl4, dl5 and dl6 domains as well as their dorsal shift in position.

Antagonistic Gradients

Loss of either Wnt or BMP signals results in dorsally expanded expression of ventral transcription factors and neurons, suggesting that these dorsally secreted signals establish an antagonistic gradient against Hh, although it is still unclear exactly how this occurs. Some of what is known is that Shh can antagonize the level of BMPs by inducing ventral neural tube expression of follistatin, chordin and noggin, secreted antagonists of BMPs. In the ventral spinal cord Wnt inhibitors regulate transcription of Hh-responsive genes (Lei et al., 2006) whereas in dorsal spinal cord Gli3 repressor inhibits Wnt signaling (Ulloa et al., 2007). Some of these antagonistic relationships have also been shown to exist outside the spinal cord. Within the epithelium of the colon, high levels of Wnt signaling are restricted to the base of the proliferative crypt by Ihh, expressed by mature colonocytes, and Ihh reciprocally inhibits expression of Wnt target genes (van den Brink et al., 2004). Studies in the cerebellum suggest Wnt1 induces the transcription factor growth-arrest specific gene 1 (*Gas1*), which has been shown to form a physical complex with the N terminus of Shh (Lee et al., 2001).

Zebrafish as a Model System

Brachydanio rerio, a tropical fresh water jawed fish, was first reported by Francis Hamilton in 1822 in his book "Account of the fishes in the River Ganges and its Branches." In the 1960's this fish, commonly referred to as zebrafish, became the interest of George Streisinger to "study features of the organization

and embryological development of the vertebrate nervous system through the use of mutant strains," G. Streisinger, 1974 supplemental grant application to the National Science Foundation (Grunwald and Eisen, 2002). He picked zebrafish, first, because of their easy maintenance within a laboratory and because a female could easily give rise to hundreds of offspring within one clutch. Second, embryonic development occurs quickly and because zebrafish fertilize embryos externally this can be easily observed via live imaging. For example, within 10 hours post fertilization (hpf) the embryo has established its dorsal and ventral axis and begun its anterior-posterior elongation (Figure 1.9 A, Figure 1.9 modified from Kimmel et al. 1995). Less than ten hours later muscular twitches can be seen, almost all of the somites are formed and structures such as the eyes, otic vesicle (ear) and hindbrain are apparent (Figure 1.9 B). By 24 hpf the heartbeat is detectable and the cerebellar anlage is present, this usually does not occur until Embryonic (E) day 9 in mice, another commonly studied vertebrate system. By 48 hpf, beginning the larval stage, the embryo will have pigmentation and begin to hatch out of its transparent chorion (egg) (Figure 1.9 C). By 3 days post fertilization (dpf) the protruding jaw can be seen accompanied by a decrease in the size of the yolk preparing the embryo to eat on its own by 5 dpf by using its newly formed swim bladder. (Figure 1.9 D, E).

Zebrafish also present a unique opportunity to perform large scale screens in a vertebrate system using forward genetics, a method in which the observation of an abnormality in its physical appearance or a trait (phenotype) is identified first, followed by characterization of the gene(s) responsible for causing the
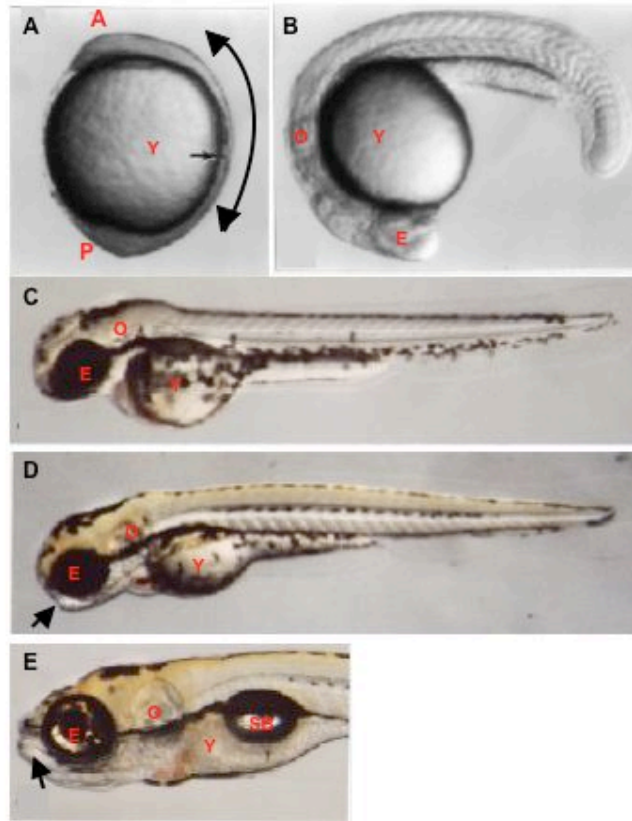
Figure 1.9. *Images of live development modified from ZFIN.* All panels are whole mount images. Black arrows indicate jaw. Anterior (A), Posterior (P), Yolk (Y), Eye (E), Otic vesicle (O), Swim Bladder (SB). (A) A WT embryo at 10 hpf undergoing elongation along the AP axis. (B) By 20 hpf the eye and otic vesicle are readily visible. (C) Pigmentation is evident in the eye and along the body by 48 hpf. (D) By 3 dpf the jaw has not yet fully protruded, however by 5 dpf (E) the jaw is extended and the swim bladder is formed.

defect. The first large scale screens using forward genetics were published in Development in December 1996 and had such a large impact that the entire journal (all 37 articles) were dedicated to reporting the approximately 4,000 embryonic-lethal mutants that were characterized in this screen. Use of transgenics allows for examination of effects on specific cell types, which can be identified with stable fluorescent proteins, and to create temporally inducible methods to express and block gene function. Transgenics, in combination with mutants and easy manipulation of embryos by pharmacological agents has catapulted zebrafish as a mainstream vertebrate system for scientific research.

Neuronal Circuitry of Zebrafish Cerebellum Versus Mammalian

Many of the cell types and circuits that exist in the mammalian cerebellum are conserved in the zebrafish cerebellum. One difference however, is that in teleosts there are no deep cerebellar nuclei, usually the target of PNs. Instead, PNs are thought to either project directly to the brain area they are targeting or onto eurydendroid neurons, efferent neurons that serve a similar function to deep cerebellar nuclei (Figure 1.10). In mammals, antibody specific to calbindin, a Calcium (Ca) channel antibody is used to identify all PNs, however, in teleosts calbindin does not identify PNs. Instead calretinin, a similar antibody to calbindin identifies eurydendroid neurons (Castro et al., 2006; Diaz-Regueira and Anadon, 2000). In zebrafish cerebellum anti-Zebrin II antibody and *olig2* expression identify subsets of Purkinje neurons (Ikenaga et al., 2006; Lannoo et al., 1991a; Lannoo and Hawkes, 1997). Overall the circuitry is highly similar even though the
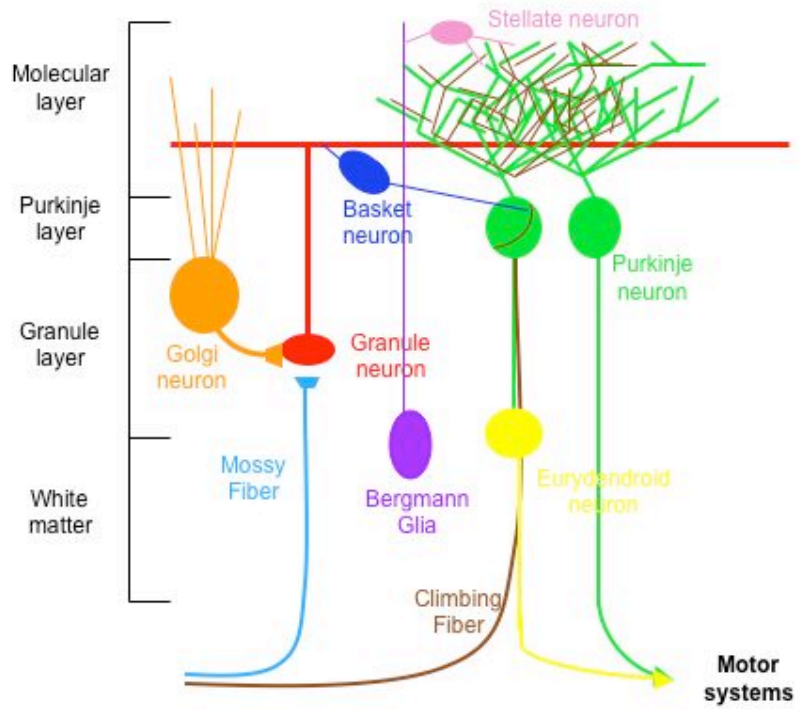
Figure 1.10. *Schematic diagram representing zebrafish cerebellum neuronal circuitry.* Note the absence of deep cerebellar nuclei and the addition of eurydendroid neurons.

telostean cerebellar structure is simplified. However, many of the cell types and functions of these cell types are conserved. In mammals PNs are arranged in alternating Zebrin II$^+$ and Zebrin II$^-$ parrasagital stripes. Zebrin II positive and negative PNs are also compartmentalized in fish, but the compartmental arrangement is somewhat different. Interestingly, these studies reveal that Zebrin II$^-$ PNs are generally medial and ventral to Zebrin II$^+$ PNs, similar to our findings for the zebrafish cerebellum at early larval stages. Furthermore, the neurons expressing Zebrin II, *olig2* and Calretinin have the same relationship described for intrinsic PNs, projection PNs and eurydendroid neurons described in previous work (Brochu et al., 1990; Lannoo et al., 1991b).

Function of the Cerebellum

Surgical removal of the cerebellum from live animals by Luigi Rolando in the late 18th century produced some of the first evidence that the cerebellum is the control center for motor function (Dow, 1958; Fine et al., 2002). Later studies repeating Rolando's work in 1924 by Flourens in addition to Sir Gordon Holmes' study of effects of gun shot wounds to the cerebellum, established the cerebellum has a critical role in coordination of movements as well as balance (Holmes, 1939; Morton and Bastian, 2004). Recent studies also suggest cognitive learning skills, language and emotional processing as additional functions of the cerebellum (Holmes, 1939; Ito, 2000; Raymond et al., 1996; Schutter and van Honk, 2005; Thach et al., 1992). Many of these functions of the cerebellum are conserved from human to teleost. In addition to motor control, a

recent study even suggests the teleost cerebellum contributes to conditional learning as well as emotional functions as evident by both conditional and fear response tests (Rodriguez et al., 2005).

Disease Implications

The signaling pathways that are required to establish a functioning system are often the same ones that go awry and cause cancer and growth of tumors. The cerebellum is no exception. Many tumors such as medulloblastomas, astrocytomas and ependymomas form within the cerebellum of children due to abnormalities during cerebellar development (Lechtenberg, 1993). Specifically, over expression of Shh has been directly linked to medulloblastomas, causing over-proliferation of granule neurons to begin tumor formation. In addition, degenerative diseases such as spinocerebellar ataxia and Friedreich's disease, as well as demyelinating diseases including multiple sclerosis (MS), involve the cerebellum and thus motor coordination and cognition (Geschwind, 1999; White et al., 2000). A comprehensive understanding of the organization of neuronal circuitry and the signals regulating the overall formation and function of the cerebellum must be characterized to better design therapeutic strategies targeting cerebellar pathologies.

While much work has been devoted to understanding the later processes of cerebellar organization, the early roles these major pathways have during cerebellar development are still not understood. Insight into their role earlier in development may provide important clues as to why they go awry later in life.

Using a simple model like zebrafish allows us to examine embryonic development of the cerebellum that has previously been primarily overlooked. One caveat to these studies has been the inability to uniquely identify multiple cerebellar cell types in the zebrafish. However our finding that *olig2* expression identifies a subset of PNs has enabled us to examine the DV patterning of the cerebellum and the pathways critical to this process.

CHAPTER II

HH AND WNT SIGNALING REGULATE FORMATION OF *OLIG2*$^+$ PURKINJE NEURONS IN THE ZEBRAFISH CEREBELLUM

Abstract

The cerebellum, which forms from anterior hindbrain, coordinates motor movements and balance. Sensory input from the periphery is relayed and modulated by cerebellar interneurons, which are organized into layers. The mechanisms that specify the different neurons of the cerebellum and direct its layered organization remain poorly understood. Drawing from investigations of spinal cord, we hypothesized that the embryonic cerebellum is patterned on the dorsoventral axis by opposing morphogens. We tested this using zebrafish. Here we show that expression of *olig2*, which encodes a bHLH transcription factor, marks a subset of PNs. In combination with other markers, *olig2* reveals a dorsoventral organization of cerebellar neurons in embryos. Disruption of Hedgehog signaling, which patterns the ventral neural tube, produced a two-fold increase in the number of *olig2*$^+$ PNs. By contrast, *olig2*$^+$ PNs did not develop in embryos deficient for Wnt signaling, which patterns dorsal neural tube, nor did they develop in embryos deficient for both Hedgehog and Wnt signaling. Our data indicate that Hedgehog and Wnt work in opposition across the dorsoventral axis of the cerebellum to regulate formation of *olig2*$^+$ PNs. Specifically, we propose that Hedgehog limits the range of Wnt signaling, which is necessary for *olig2*$^+$ PN development.

Introduction

The cerebellum functions as the main control center for balance and motor function and also contributes to cognitive learning (Fiez, 1996; Holmes, 1939; Ito, 2000; Morton and Bastian, 2004; Raymond et al., 1996; Schutter and van Honk, 2005; Thach et al., 1992). It is radially organized into several distinct layers, which are interconnected by axonal projections and synaptic contacts (Altman and Bayer, 1978; Altman and Bayer, 1985; Wang and Zoghbi, 2001). The molecular layer is the outermost and consists of stellate and basket neurons, which make synaptic connections with dendrites of Purkinje neurons (PN). Golgi cells and the cell bodies of PNs comprise the Purkinje layer, just below the molecular layer. PNs are the chief output neuron of the mammalian cerebellum and their axons project to deep cerebellar nuclei (Altman and Bayer, 1985), which relay signals to various output peduncles that synapse with midbrain structures (thalamus, red nuclei and premotorcortex), dorsal brainstem or cerebral neocortex (de Zeeuw and Berrebi, 1996). The granule layer, located below the Purkinje layer, consists of granule neurons, which are excitatory cells that also synapse with PN dendrites. In teleosts, some PNs project directly onto eurydendroid neurons, located ventral to PN cell bodies, which in turn make connections to the diencephalon and caudal medulla and serve the same function as deep cerebellar nuclei in mammalian systems (Diaz-Regueira and Anadon, 2000; Ikenaga et al., 2006; Lannoo et al., 1991b). Other PNs provide direct output to motor nuclei and various brain regions, which often terminate in multiple brainstem nuclei (Ikenaga et al., 2005; Luiten and van der Pers, 1977).

Of these cerebellar features, the development of granule neurons is

perhaps best understood. Granule neuron progenitors arise from the rhombic lip,

a specialized proliferative zone along the dorsolateral rhombencephelon. Guided,

at least in part, by Netrin1 and Slit2, they migrate over the surface of the

cerebellum to form a transient external granule layer (Gilthorpe et al., 2002)

Subsequently, signals secreted by PNs cause granule neuron progenitors to

proliferate and migrate into the cerebellum to form the inner granule layer

(Dahmane and Ruiz i Altaba, 1999; Traiffort et al., 1998).

All other neurons of the cerebellum apparently originate within the

proliferative ventricular zone (VZ). Deep cerebellar neurons are produced first,

followed by PNs and then stellate, basket and Golgi neurons (Altman and Bayer,

1978; Altman and Bayer, 1985). Retrospective lineage analysis in mouse and

chick showed that whereas some small clones consisted only of deep cerebellar

neurons (Mathis and Nicolas, 2003), other clones included PNs, molecular layer

neurons and glia (Lin and Cepko, 1999; Mathis et al., 1997). Thus, many

cerebellar VZ precursors are multipotent, producing distinct cell types that

occupy different layers. Although several genes that are important for PN

migration and maintenance have been described (Wang and Zoghbi, 2001), very

little is known about the mechanisms that specify cerebellar cell type and

determine the layered organization of the cerebellum.

Here we describe experiments designed to investigate mechanisms of

cerebellar patterning during development, using zebrafish as a model system.

We hypothesized that signals that pattern the dorsoventral (DV) axis of the

neural tube influence the fate of cells that arise from the cerebellar VZ, similar to neuronal specification in the spinal cord. Consistent with this, we found that Hedgehog (Hh) signaling, which is active in ventral neural tube, limits the number of a subset of PNs that express *olig2*. Expansion in Purkinje cell number resulting from loss of Hh signaling was accompanied by an expansion of *wnt1* expression. Conversely, embryos deficient for Wnt signaling failed to form *olig2*[+] PNs, even in the absence of Hh signaling. Our data support a model in which Wnt signaling, limited to dorsal cerebellum by Hh, is necessary for *olig2*[+] PN specification.

Materials and methods

Zebrafish staging and strains

Embryos were produced by pair wise matings and raised at 28.5°C, then staged according to hours post fertilization (hpf) and days post fertilization (dpf) in addition to morphological criteria (Kimmel et al., 1995). Mutant alleles included *smo*[b641] (Barresi et al., 2000; Varga et al., 2001) and *Df(LG01:lef1)*[x8] (Phillips et al., 2006). Transgenic alleles included *Tg(olig2:egfp)*[vu12] (Shin et al., 2003) and *hsDkk1GFP* (Stoick-Cooper et al., 2007).

In situ RNA hybridization

In situ RNA hybridization was performed as described previously (Hauptmann and Gerster, 2000). Antisense RNA probes included *olig2* (Park et al., 2002), *ptc1* (Concordet et al., 1996), *shh* (Krauss et al., 1993), *atoh1a* (Kim et

al., 1997) and *wnt1* (Molven et al., 1991). Hybridization was detected using anti-digoxigenin antibody conjugated to alkaline phosphatase, followed by a color reaction using a solution of BM Purple AP Substrate (Roche Diagnostics). All embryos for sectioning were embedded in 1.5% agar/5% sucrose and frozen in 2-methyl-butane chilled by immersion in liquid nitrogen. Sections of 10 µm thickness were obtained using a cryostat microtome. Whole embryos were de-yolked for imaging and placed in 75% glycerol solution on bridged slides and coverslipped. Images were collected using a QImaging Retiga Exi color CCD camera mounted on an Olympus AX70 compound microscope and imported into Adobe Photoshop. All image manipulations were restricted to adjustment of levels, curves, saturation and hue.

Immunohistochemistry

We used the following primary antibodies for immunohistochemistry on fixed embryos: mouse anti-Zebrin II (1:1000, gift of Dr. R Hawkes) (Brochu et al., 1990), mouse anti-HuC/D (16A11, 1:100, Molecular Probes) (Marusich et al., 1994) and rabbit anti-calretinin (1:1000, Swant Products) (Schwaller et al., 1993). For fluorescent detection we used Alexa Fluor 568 goat anti-mouse conjugate and Alexa Fluor 647 goat anti-rabbit (1:200, Molecular Probes). All embryos for sectioning were embedded in 1.5% agar/5% sucrose and frozen in 2-methyl-butane chilled by immersion in liquid nitrogen. Sections of 10 µm thickness were obtained using a cryostat microtome. Fluorescent images of sectioned embryos were collected using a 40X oil-immersion (NA = 1.3) objective mounted on a

33

motorized Zeiss Axiovert 200 microscope equipped with a PerkinElmer ERS spinning disk confocal system or a Zeiss LSM510 Meta laser scanning confocal microscope and imported into Volocity (Improvision). Whole mount fluorescent images were collected using a QImaging Retiga Exi color CCD camera mounted on an Olympus AX70 compound microscope and imported into Adobe Photoshop. All image manipulations were restricted to adjustment of levels, curves, saturation and hue.

Cyclopamine treatments

Embryos were incubated in Embryo Medium (EM) (15 mM NaCl, 0.5 mM KCl, 1 mM CaCl2, 1 mM MgSO4, 0.15 mM KH2PO4, 0.05 mM NH2PO4, 0.7 mM NaHCO3) containing 50 µM cyclopamine (CA) (Toronto Research Chemicals), diluted from a 10 µM stock dissolved in ethanol. Embryos were treated in their chorions at shield stage or following manual dechorionation with any treatments that began after 24 hpf.

Heat-shock induction

To induce expression of Dkk1, *hsDkk1GFP* embryos were collected from matings of heterozygous *hsDkk1GFP* fish and raised in EM at 28.5ºC. Embryos were cooled to 24ºC for one hour at 29 hpf then transferred to a microfuge tube filled with EM in a 40ºC water bath for one hour. Embryos were sorted by GFP expression and only highly-expressing embryos were selected for analysis. These embryos were then placed back in EM at 28.5ºC and raised until 48 hpf.

Quantification of EGFP$^+$ Purkinje neurons

To quantify the number of EGFP$^+$ cells in a whole cerebellum *Tg(olig2:egfp)* embryos were fixed at 48 hpf. The embryos were dissected using watch maker's forceps, removing the eyes, yolk, forebrain and trunk to isolate the cerebellum. Cerebellums were mounted in 75% glycerol on bridged coverslips. Images were collected at 2 µM intervals through the entire depth of the cerebellum using a confocal microscope. The images were imported into Volocity and then exported to Openlab (Improvision). Each Z stack image was examined and individual EGFP$^+$ cells were labeled and counted.

Results

Zebrafish cerebellar cells express olig2

To initiate an investigation of cerebellar patterning we examined expression of *olig2*, which encodes a bHLH transcription factor (Lu et al., 2000; Park et al., 2002; Takebayashi et al., 2000; Zhou et al., 2000), by in situ RNA hybridization. At 24 hours post fertilization (hpf), expression was evident in ventral spinal cord, as previously described (Park et al., 2002), and in ventral diencephalon but not in the cerebellum (Figure 2.1 A). By 36 hpf, a prominent domain of *olig2* expression appeared near the dorsal boundary between midbrain and hindbrain (data not shown). Expression was maintained at 48, 72, and 96 hpf (Figure 2.1 B-D) through at least 7 days post fertilization (dpf) (data not shown). Transverse and sagital tissue sections revealed that cerebellar cells
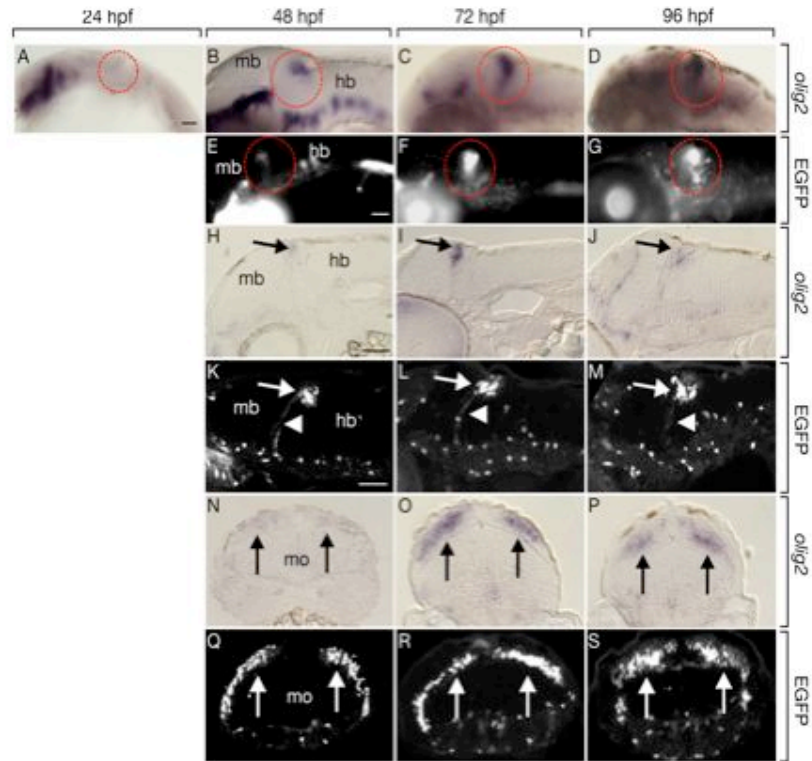
Figure 2. 1. *Transgenic reporter gene expression recapitulates endogenous olig2 RNA expression in zebrafish cerebellum.* Lateral whole mount views and sagital sections are shown with dorsal up and anterior to the left. Transverse sections are oriented dorsal up. Midbrain (mb), hindbrain (hb) and medulla oblongata (mo) are marked. (A-D) Developmental time course of *olig2* expression detected by in situ RNA hybridization in whole embryos. Dashed circles mark where cerebellum is located. (E-G) EGFP expression driven by the *Tg(olig2:egfp)* transgene in live embryos. Expression within cerebellum is circled. (H-J) Sagital sections through cerebellum with *olig2* RNA expression marked by arrows. (K-M) Arrows mark EGFP^{+} cells in cerebellum of sagitally sectioned *Tg(olig2:egfp)* embryos and arrowheads show axonal extensions from EGFP^{+} cells. Transverse sections through cerebellum showing *olig2* RNA (N-P) and EGFP (Q-S) expression marked by arrows. Scale bars represent 20 µm in all panels.

dorsal to the anterior medulla oblongata expressed *olig2* (Figure 2.1 H-J, N-P) in a pattern consistent with that of other cerebellar genes (Mueller et al., 2006; Mueller and Wullimann, 2003).

Previously, we described a transgenic line in which *olig2* regulatory DNA drives expression of EGFP, recapitulating endogenous *olig2* expression in spinal cord (Shin et al., 2003). The pattern of cerebellar EGFP expression was also identical to that of *olig2* RNA (Figure 2.1 E-G, K-M, Q-S), with the exception that EGFP was first detectable at 40 hpf, presumably reflecting a delay in EGFP folding and fluorescence following translation (data not shown). EGFP in *Tg(olig2:egfp)* embryos is cytosolic and reveals both cell bodies and processes. Notably, EGFP$^+$ cells extended long axonal processes, characteristic of PNs, to the deep brainstem.

olig2 expression identifies a subset of PNs

To determine the identity of cerebellar *olig2*$^+$ cells we labeled sagital sections of *Tg(olig2:egfp)* embryos with anti-Hu antibody, which identifies newly born postmitotic neurons (Marusich et al., 1994). The majority of the cerebellar EGFP$^+$ cells expressed Hu, identifying them as neuronal (Figure 2.2 A-C). High magnification dorsal views of living *Tg(olig2:egfp)* embryos revealed deep ventral projections, as noted above, as early as 54 hpf and extensive dendritic arbors by 7 dpf (Figure 2.2 D,E). As with the axonal projections, these dendritic arborizations are characteristic of PNs. To further characterize EGFP$^+$ cells, we
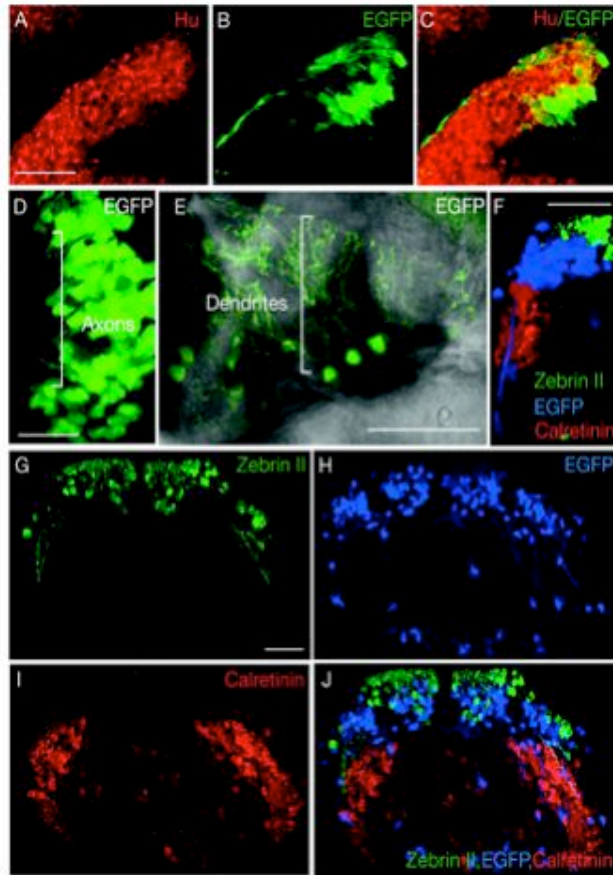
Figure 2.2. *olig2 expression identifies a subset of Purkinje neurons.* (A-C) Sagital section through cerebellum of 48 hpf *Tg(olig2:egfp)* transgenic embryo showing EGFP⁺ cells express Hu. (D) Dorsal view with anterior to left of one half of the cerebellum in living *Tg(olig2:egfp)* embryo at 56 hpf. Bracket marks EGFP⁺ axons extending from EGFP⁺ cells ventrally along midbrain-hindbrain boundary. (E) Dorsal view of cerebellum in living *Tg(olig2:egfp)* embryo at 7 dpf, anterior is along the bottom. Bracket indicates extensive dendritic branches originating from EGFP⁺ cells. (F-J) Sections through cerebellum of *Tg(olig2:egfp)* embryos labeled with Zebrin II and Calretinin antibodies. (F) 3-D reconstruction of sagital section illustrating DV organization of Zebrin II⁺, EGFP⁺ and Calretinin⁺ cells. (G-H) Transverse section showing Zebrin II, EGFP and Calretinin labeling. (J) Merged image. Scale bars represent 20 μm in all panels.

labeled transverse and sagital sections of 5 dpf *Tg(olig2:egfp)* embryos with

Zebrin II antibody, which identifies a subset of PNs in both mammals and teleosts

(Brochu et al., 1990; Lannoo et al., 1991a; Lannoo et al., 1991b; Meek et al.,

1992). EGFP and Zebrin II immunoflourescence did not colocalize (Figure 2.2 F-

H, J) indicating that these markers reveal distinct subsets of PNs. Although some

EGFP$^+$ and Zebrin II$^+$ cells were intermixed, most EGFP$^+$ cells were ventral to

Zebrin II$^+$ cells (Figure 2.2 F, J). We then immunolabeled *Tg(olig2:egfp)* embryos

with antibody specific to Calretinin, a calcium-binding protein expressed by

eurydendroid neurons (Castro et al., 2006; Diaz-Regueira and Anadon, 2000).

Calretinin$^+$ eurydendroid neurons were positioned ventrally to EGFP$^+$ and Zebrin

II$^+$ PNs (Figure 2.2 F, I, J). Together, these data reveal a DV organization of the

zebrafish cerebellum, with eurydendroid neurons, *olig2$^+$* PNs, and Zebrin II$^+$ PNs

occupying ventral, intermediate and dorsal positions, respectively.

The olig2$^+$ PN population is enlarged in the absence of Hh signaling

      In the spinal cord, specification of different cell types along the DV axis is

influenced by graded Hh signaling (Jessell, 2000). Ventral spinal cord cells in

mouse and zebrafish embryos that lack Hh signaling failed to express *olig2* (Lu et

al., 2000; Park et al., 2002), indicating Hh promotes *olig2* expression. To test the

possibility that Hh also patterns the cerebellar DV axis, we investigated *olig2*

expression in embryos that were homozygous for a mutation of the *smoothened*

(*smo*) gene, which encodes a seven transmembrane protein necessary for Hh

signaling (Alcedo et al., 1996; Huangfu and Anderson, 2006). As previously

described (Park et al., 2002), spinal cord cells of *smo* mutant embryos did not express *olig2* (Figure 2.3 D). By contrast, cerebellar *olig2* expression was elevated in *smo* mutant embryos (Figure 2.3 A-F). From a dorsal view, the stripe of *olig2* expression was both broader in the anteroposterior axis and extended more ventrally than normal (Figure 2.3 B, C, E, F).

To quantify cerebellar *olig2*^{+} cells, we used confocal microscopy to count EGFP^{+} cells of *Tg(olig2:egfp)* embryos. At 48 hpf, an average of approximately 65 EGFP[+] PNs occupied each half of the cerebellum of wild-type transgenic embryos (Figure 2.4 A). Similarly staged *smo^{-/-};Tg(olig2:egfp)* embryos had nearly a two-fold increase in the number of EGFP^{+} cells (Figure 2.4 A). Thus in normal development, Hh limits formation of *olig2*[+] PNs.

Previous studies have shown the pharmacological agent CA directly binds to Smoothened and specifically inhibits Hh signal transduction (Chen et al., 2002). Consistent with this, zebrafish embryos incubated with CA had a deficit of motor neurons, similar to *smo* mutant embryos (Chen et al., 2001; Lewis and Eisen, 2001; Park et al., 2004). To determine if CA treatment phenocopies the *smo* mutant cerebellar defect, we treated *Tg(olig2:egfp)* embryos at 6 hpf, an early gastrulation stage, and counted EGFP^{+} cells as described above (Figure 2.4 A). Similar to *smo* mutant embryos, CA treated embryos had a two-fold increase in EGFP[+] cell number when compared to control embryos.

To determine the time during which Hh signaling is necessary for regulating *olig2*[+] PN formation, we utilized CA to selectively block Smoothened function at different intervals. We treated *Tg(olig2:egfp)* embryos at 24, 28, 32,
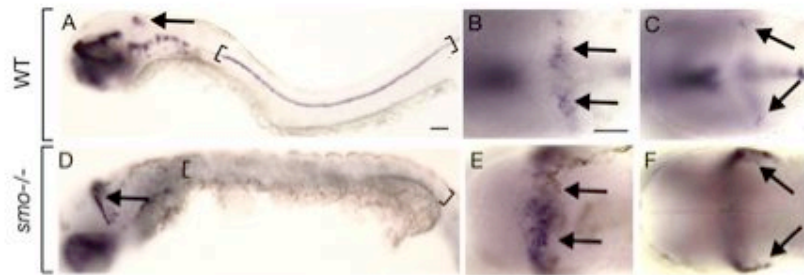
Figure 2.3. *Hh signaling restricts cerebellar olig2 expression.* Lateral (A, D) and dorsal (B, C, E, F) views of 48 hpf embryos with anterior to the left. Arrows indicate cerebellar *olig2* expression. Brackets mark ventral spinal cord. (A) Wild-type embryo illustrating *olig2* expression within cerebellum and spinal cord. Dorsal (B) and ventral (C) focal planes of wild-type cerebellum. (D-F) Similar views of *olig2* expression in *smo* mutant embryo. Note expansion of cerebellar expression and absence of spinal cord expression. Scale bars represent 20 μm for all panels.
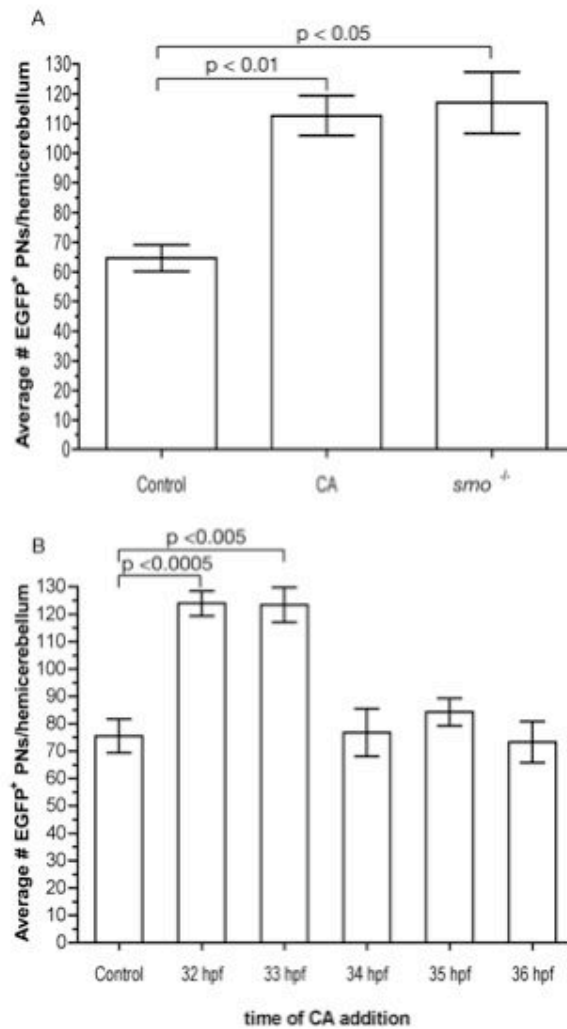
Figure 2.4. *Temporal regulation of olig2+ PN number by Hh signaling.* (A) Graph depicting average number of EGFP+ cerebellar cells. n = 14 hemicerebellums for each condition. Statistical significance calculated in accordance to student T test. (B) Time course assay of EGFP+ cells in *Tg(olig2:egfp)* embryos treated with CA. 32 and 33 hpf treatments produced significant increases compared to control. n= 10 hemicerebellums for each time point except 35 hpf, where n=11.

33, 34, 35, and 36 hpf, allowed them to mature to 48 hpf and counted EGFP^{+} cells as described above. Embryos treated at 33 hpf and earlier had approximately the same number of EGFP^{+} cerebellar cells as *smo* mutant embryos and embryos treated continuously from 6 hpf with CA. By contrast, those treated at 34 hpf and later had approximately the same number as control embryos (Figure 2.4 B). These data indicate Hh signaling regulates *olig2*[+] PN development before 33 hpf.

Expression patterns of Hh pathway genes do not coincide with olig2[+] PNs

To investigate if Hh signaling is active in cerebellar cells we used in situ RNA hybridization to analyze expression of genes that encode components of the Hh pathway. *shh* expression was ventral to the cerebellum at 30 hpf and 48 hpf (Figure 2.5 A-C), spanning the critical time period for Hh regulation of *olig2*[+] PN formation. As previously reported (Ekker et al., 1995) *tiggy winkle hedgehog* (*twhh*) was expressed similarly to *shh*, whereas *echidna hedgehog* (*ehh*) was restricted to the trunk notochord (Currie and Ingham, 1996) (data not shown). *patched 1* (*ptc1*) RNA, which is expressed by cells in which the Hh pathway is active, (Concordet et al., 1996; Marigo and Tabin, 1996), was prominent along the rhombic lip of the hindbrain but not within the cerebellum (Figure 2.5 D-F). *gli1*, which encodes a transcription factor that mediates Hh signaling (Karlstrom et al., 2003; Lee et al., 1997), was expressed similarly to *ptc1* (data not shown). Thus, although our functional data show that Hh signaling limits formation of *olig2*[+] PNs, our gene expression data indicate that Hh signaling is active only in
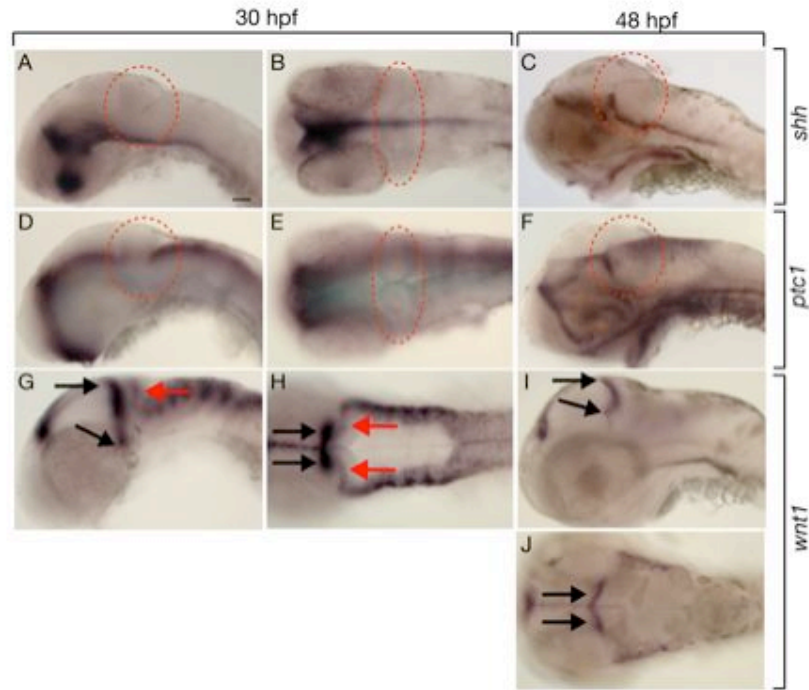
43

Figure 2. 5. *Zebrafish cerebellum expresses wnt1 but not Hh pathway genes.*
All panels are lateral or dorsal views with anterior to the left. Dashed circles
mark cerebellums. (A-C) Expression of *shh* is ventral to cerebellum. (D, E)
Expression of *ptc1* at 30 hpf is absent from cerebellum. (G, H) Gene
expression of *wnt1* at 30 hpf, red arrows mark transient *wnt1* expression within
the cerebellum while black arrows mark expression at the midbrain hindbrain
boundary. By 48 hpf expression is no longer present within the cerebellum and
expression at midbrain hindbrain boundary is ventrally restricted (I, J). Scale
bars represent 20 µm in all panels.

cells located at a distance from the site of PN formation. This raised the possibility that Hh signaling influences PN development indirectly, by regulating other pathways.

Spinal cord patterning and specification of neurons along the DV axis is dependant on opposing gradients of morphogens secreted from the roof plate and floor plate (Wilson and Maden, 2005). Notably, dorsal spinal cord and roof plate cells secrete Wnt1 and Wnt3a (Lee and Jessell, 1999; McMahon and Bradley, 1990; Roelink and Nusse, 1991). To investigate whether *wnt1* is a candidate to regulate PN development, we examined its expression using in situ RNA hybridization. At 30 hpf there were two domains of *wnt1* expression close to the cerebellum. The first domain included cells along the dorsal midbrain, extending ventrally at the midbrain-hindbrain boundary. The second domain, marked by a relatively low level of *wnt1* transcripts, included the dorsal cerebellum (Figure 2.5 G, H). At 48 hpf expression near the midbrain-hindbrain boundary remained strong whereas *wnt1* transcripts were no longer evident in dorsal cerebellum (Figure 2.5 I, J). Thus, cerebellar *wnt1* expression coincides with the critical period for Hh regulation of PN formation.

Wnt signaling is necessary for olig2$^+$ PN development

We tested whether Wnt signaling regulates formation of PNs by investigating *olig2* expression. Lymphoid enhancer 1 (Lef1) mediates nuclear response to Wnt signals and functions as a transcriptional activator in the presence of β-catenin (Clevers and van de Wetering, 1997). The chromosomal

deficiency *Df(LG01:lef1)^{x8}* deletes approximately 2-8 cM of Linkage Group 1,

spanning the *lef1* locus (Phillips et al., 2006). In situ RNA hybridization revealed

that, in contrast to *smo* mutants, *Df(LG01:lef1)^{x8}* mutant cerebellar cells failed to

express *olig2* at 48 hpf whereas spinal cord expression was normal (Figure 2.6

D-F). Because Wnt signaling has an earlier role in forming the midbrain-hindbrain

boundary (Bally-Cuif et al., 1995; Kelly and Moon, 1995) and the *Df(LG01:lef1)^{x8}*

deletion removes additional genes, we used a heat-shock activated transgenic

line, *hsDkk1GFP,* to conditionally express the Wnt inhibitor Dkk1. Dkk1 is a

secreted ligand for LRP6, a coreceptor necessary for Wnt signal transduction

(Liu et al., 2003; Semenov et al., 2001). LRP6 preferentially binds to Dkk1 in the

presence of Wnt, prohibiting it from forming a complex with the Frizzled receptor

and preventing pathway activation. We induced expression of Dkk1 using heat

shock at 30 hpf and examined *olig2* expression at 48 hpf using in situ RNA

hybridization. Similar to *Df(LG01:lef1)^{x8}* mutant embryos, transgenic heat-

shocked embryos expressed *olig2* in spinal cord but not cerebellum (Figure 2.6

J-L). These data indicate Wnt signaling is necessary for *olig2^{+}* PN formation.

Our data raised the possibility that Hh signaling limits the range of Wnt

activity, which is necessary for *olig2^{+}* PN formation. Thus, we predicted that the

absence of Wnt would be epistatic to loss of Hh signaling. To test this we treated

Df(LG01:lef1)^{x8} mutant embryos with CA at 6 hpf and examined *olig2* expression

at 48 hpf. As expected, spinal cord cells of these mutants did not express *olig2*

in the absence of Hh (Figure2.6 I). Notably, cerebellar cells also did not express

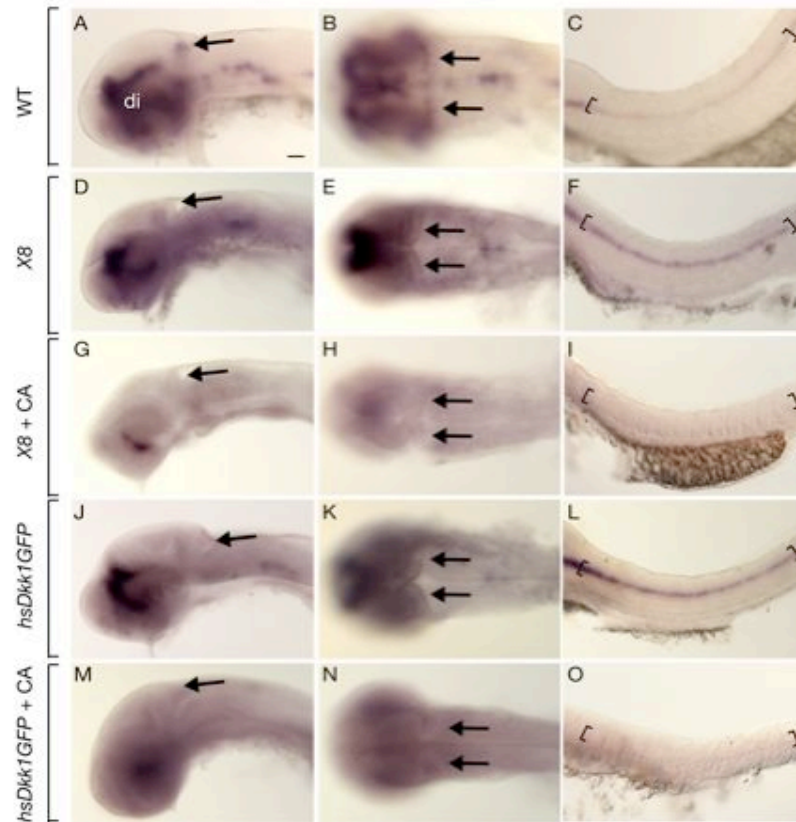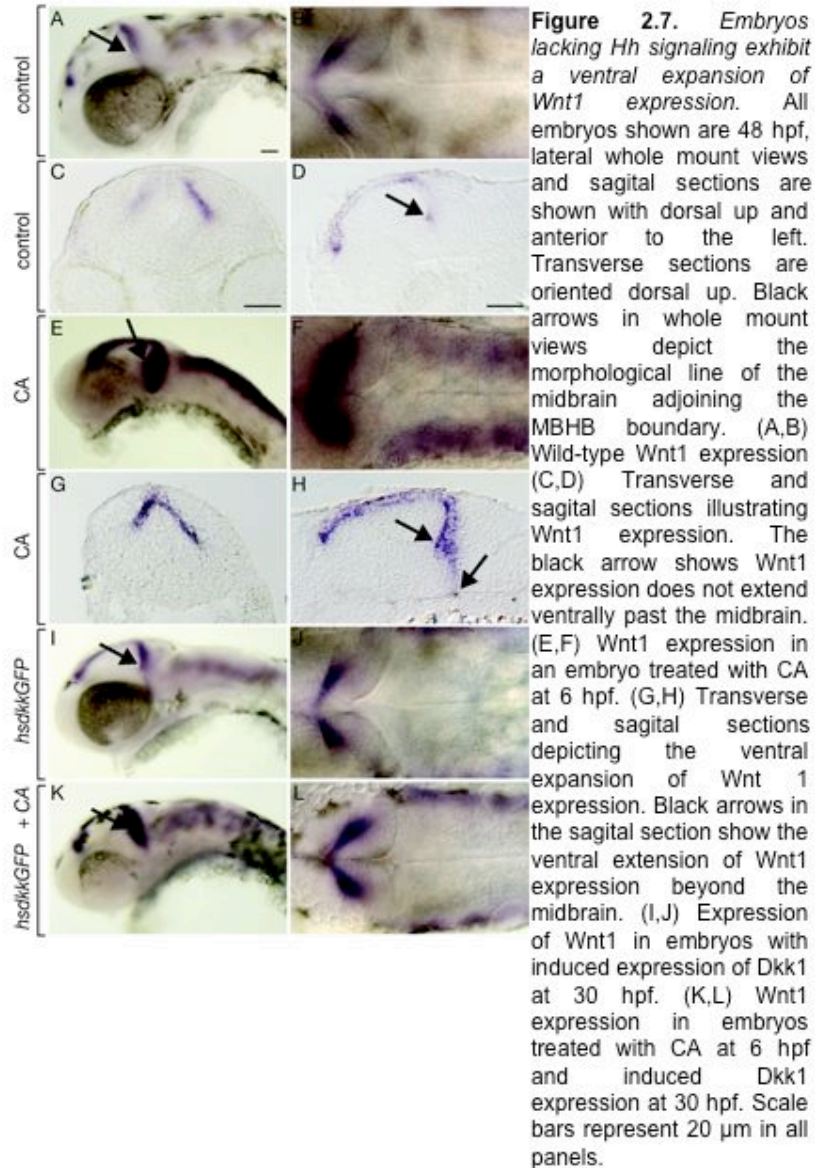*olig2* (Figure 2.6 G, H). Similarly, heat shock induction of Dkk1 at 30 hpf entirely

46

Figure 2.6. *Wnt signaling is necessary for cerebellar olig2 expression.* All embryos shown are 48 hpf. Anterior is to the left in all panels, the first column depicts a lateral whole mount view, the second column a dorsal view and the third a lateral view of the spinal cord. Black arrows mark cerebellum, brackets mark ventral spinal cord and ventral diencephalon is labeled (di). (A-C) Wild-type *olig2* expression. (D-F) *Df(LG01:lef1)ˣ⁸* (X8) mutant embryos expressed *olig2* in spinal cord but not cerebellum. (G-I) *Df(LG01:lef1)ˣ⁸* mutant embryos treated with CA at 6 hpf expressed *olig2* in ventral diencephalon but not cerebellum or spinal cord. (J-L) *hsDkk1GFP* embryos heat shocked at 30 hpf expressed *olig2* in ventral diencephalon and spinal cord but not cerebellum. (M-O) *hsDkk1GFP* embryos treated with CA at 6 hpf expressed *olig2* in ventral diencephalon but not spinal cord or cerebellum. Scale bars represent 20 μm in all panels.

blocked formation of *olig2*[+] PNs in transgenic embryos treated with CA at 6 hpf (Figure 2.6 M-O). Expression of *atoh1a*, which marks the rhombic lip, appeared normal in *Df(LG01:lef1)*[x8] mutant embryos and transgenic embryos in which Dkk1 expression was induced at 30 hpf (Figure 2.8 E-H), indicating that the cerebellar primordium was intact. Thus, absence of *olig2*^{+} cells in these embryos was not due to the absence of a cerebellum. We conclude that expansion of PN number in the absence of Hh signaling is dependent on Wnt activity, consistent with the idea that Hh limits the range of Wnt signaling in the cerebellum.

Shh could limit Wnt signaling by restricting production of ligand or blocking cell response to ligand. To investigate these possibilities we first examined *wnt1* expression by in situ RNA hybridization. As shown above, at 48 hpf, *wnt1* is normally expressed at the midbrain-hindbrain boundary and seems to be restricted to a small number of cells. By contrast, in the CA treated embryos, *wnt1* expression was expanded both anteroposteriorly and ventrally at the midbrain-hindbrain boundary (Figure 2.7 E-H). Additionally, whereas overexpression of Dkk did not affect *wnt1* RNA expression (Figure 2.8 I, J), the *wnt1* expression domain was expanded in embryos treated with CA and overexpressing Dkk (Figure 2.8 K, L). These data suggest that Hh activity limits the range of Wnt signaling by limiting the number of cells that express *wnt1* RNA.

We also tested the effect of Wnt signaling on the range of Hh activity by examining *ptc1* expression. Whereas *ptc1* expression was not evident in the cerebellum of wild-type embryos (Figure 2.9 A, B), *ptc1* expression appeared to be expanded into the cerebellum of *Df(LG01:lef1)*[x8] mutant embryos (Figure 2.9
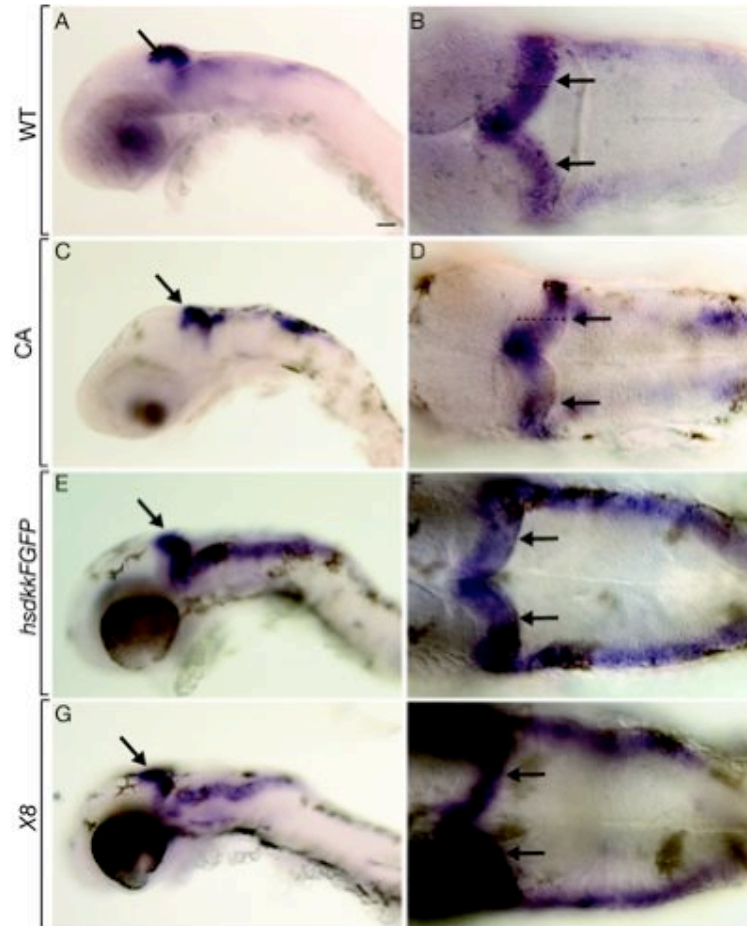
Figure 2.7. *Embryos lacking Hh signaling exhibit a ventral expansion of Wnt1 expression.* All embryos shown are 48 hpf, lateral whole mount views and sagital sections are shown with dorsal up and anterior to the left. Transverse sections are oriented dorsal up. Black arrows in whole mount views depict the morphological line of the midbrain adjoining the MBHB boundary. (A,B) Wild-type Wnt1 expression (C,D) Transverse and sagital sections illustrating Wnt1 expression. The black arrow shows Wnt1 expression does not extend ventrally past the midbrain. (E,F) Wnt1 expression in an embryo treated with CA at 6 hpf. (G,H) Transverse and sagital sections depicting the ventral expansion of Wnt 1 expression. Black arrows in the sagital section show the ventral extension of Wnt1 expression beyond the midbrain. (I,J) Expression of Wnt1 in embryos with induced expression of Dkk1 at 30 hpf. (K,L) Wnt1 expression in embryos treated with CA at 6 hpf and induced Dkk1 expression at 30 hpf. Scale bars represent 20 µm in all panels.

49

Figure 2.8. *atoh1a expression reveals a normally formed cerebellum.* All embryos shown are 48 hpf. Anterior is to the left in all panels, the first column depicts a lateral whole mount view, the second column a dorsal view. Black arrows show the cerebellum. (A,B) *atoh1a* expression in wild-type embryos. Black dashed lines indicate the width in the cerebellum (C,D) *atoh1a* expression in embryos treated with CA at 6 hpf. Black dashed line shows larger width of cerebellum. (E,F) *atoh1a* in embryos with induced expression of Dkk1 at 30 hpf. (G,H) *Df(LG01:lef1)*[x8] mutants also show normal *atoh1a* expression. Scale bars represent 20 µm in all panels.
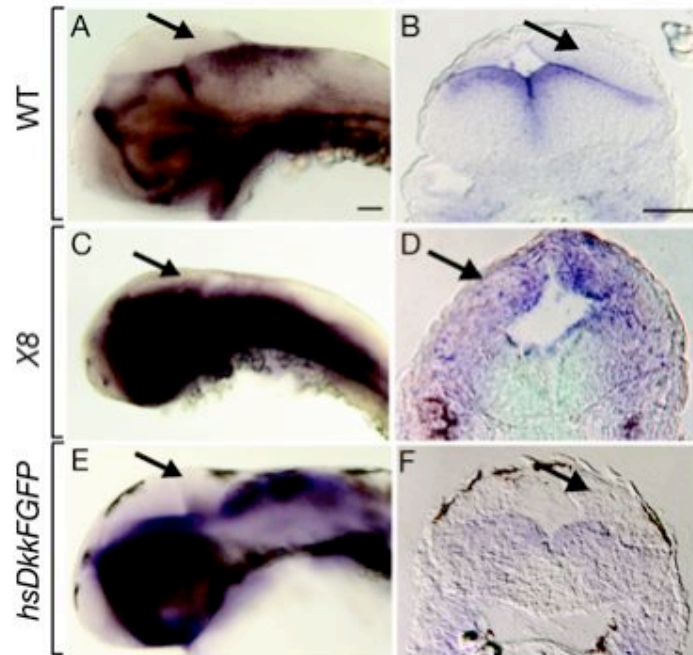
Figure 2.9. *Expansion of ptc1 expression in Df(LG01:lef1)^{x8} mutants but not in embryos with activated Dkk1 indicate two potential roles for Wnt signaling in regulating cerebellar formation.* All embryos shown are 48 hpf. The first column are whole mount views with anterior to the left the second column shows transverse sections through the cerebellum. Black arrows all point into the cerebellum. (A,B) Wild-type embryos have no *ptc1* expression within the cerebellum. (C,D) *Df(LG01:lef1)^{x8}* mutants show an expansion of *ptc1* expression into the dorsal regions of the cerebellum. (E,F) *ptc1* expression in embryos that have had Dkk1 activated at 30 hpf does not extend dorsally. Scale bars represent 20 μm in all panels.

C, D). In contrast, *ptc1* expression was not evident in the cerebellum of 48 hpf transgenic embryos in which Dkk was induced at 30 hpf (Figure 2.9 E, F). Taken together, these data raise the possibility that, prior to 30 hpf, Wnt signaling limits the range of Hh activity in the cerebellum and is later required for formation of *olig2*[+] PNs.

Discussion

olig2 expression marks a subset of Purkinje neurons and reveals cerebellar DV pattern

Despite extensive investigation of PN function, few transcription factors expressed by PNs during development have been identified (Morales and Hatten, 2006). Consequently, description of the molecules necessary for specification of PN fate remains incomplete. We noted that cerebellar cells of zebrafish embryos prominently express *olig2* RNA and EGFP driven by *olig2* regulatory sequences. EGFP^{+} cells of transgenic animals extend axons to the deep brainstem and form extensive dendritic arbors, characteristic of PNs. *Olig2* genes, which are conserved among mammals, birds and fish, encode bHLH transcription factors necessary for motor neuron and oligodendrocyte development (Lu et al., 2002; Park et al., 2002; Zhou and Anderson, 2002) but have not yet been implicated in PN development. Our data reveal *olig2* expression as a new marker of developing PNs in zebrafish and raise the possibility that *olig2* promotes PN specification or differentiation.

By comparing *olig2* expression to other markers of cerebellar cells we found evidence of a relatively simple DV organization. Cells that expressed Zebrin II, which marks a subset of PNs, were located just dorsal to *olig2*$^+$ PNs whereas Calretinin$^+$ eurydendroid neurons, which occupy the granule layer of teleosts (Castro et al., 2006; Diaz-Regueira and Anadon, 2000), were located just ventral to *olig2*$^+$ PNs. Interestingly, subdivision of PNs into Zebrin II$^+$ *olig2*$^-$ and Zebrin II$^-$ *olig2*$^+$ cells might reflect morphological and functional differences between PNs. Teleosts have at least two different kinds of PNs: those that project short axons to make synaptic contacts within the cerebellum, called intrinsic Purkinje neurons (iPNs), and those that project outside the cerebellum (pPNs) (Brochu et al., 1990; Lannoo et al., 1991b). In adults of gymnotiform and siluriform fish, Zebrin II marked both iPNs and pPNs although labeling of pPN axons was not evident during early developmental stages (Lannoo et al., 1991a). In zebrafish, eurydendroid cells, which are targets of iPN projections, are clustered along pPN axons, making it difficult to distinguish between Zebrin II labeling of iPNs and pPNs in adults (Lannoo et al., 1991a; Lannoo and Hawkes, 1997; Lannoo et al., 1991b). Our data indicate that, during development, *olig2* and Zebrin II expression distinguish between pPN and iPN populations. Whereas EGFP driven by *olig2* regulatory DNA clearly marked axons extending to the deep brainstem, we never observed Zebrin II labeling of long axons. Thus, the most dorsal subpopulation of PNs, marked by Zebrin II, might consist of iPNs whereas a more ventral subpopulation, expressing *olig2*, consists of pPNs.

Hh signaling and cerebellar patterning

Hh proteins, secreted by ventral neural tube cells and underlying notochord, function as morphogens to pattern the DV axis of the CNS (Ingham and McMahon, 2001; Jessell, 2000). This is best documented in spinal cord, where different concentrations of Shh specify distinct types of neurons that occupy different DV positions. Loss of Shh function results in loss of ventral spinal cord identity and expansion of dorsal identity (Chiang et al., 1996). Similarly, Shh is necessary for formation of dopaminergic and serotonergic neurons in the ventral midbrain and anterior hindbrain (Ye et al., 1998), indicating that its role in DV patterning extends along the entire length of the neural tube.

Hh signaling has a well established role in promoting granule neuron precursor proliferation in mice (Dahmane and Ruiz i Altaba., 1999; Corrales et al., 2004; Lewis et al., 2004) but whether it also influences PN formation is less clear. Calbindin[+] PNs were present in mice in which *Shh* or *Gli2* were conditionally inactivated in the cerebellar primordium (Blaess et al., 2006, Lewis et al., 2004; Corrales et al., 2004). However, the distribution of PNs was somewhat altered and they occupied slightly broader layers in mutant animals compared to wild type, reminiscent of the broadened domain of *olig2*[+] PNs we observed in zebrafish embryos deficient for Hh signaling. However, in contrast to our own findings, *Shh* conditional mutants had progressively fewer PNs than wild-type mice when compared from E18.5 into adulthood (Lewis et al., 2004). The progressive decrease in cell number suggests that PNs were lost due to lack

of trophic support by the diminished granule cell population of these mice, leaving the possible role of Hh in the initial formation of PNs an open question.

Our data raise the possibility that in zebrafish Hh signaling regulates DV pattern of the cerebellum. We found that *smo* mutant embryos had a morphologically distinct cerebellum and that the *olig2* expression domain appeared to be broader in the anteroposterior axis and to extend more ventrally. Quantification of *olig2*^{+} cells using a transgenic reporter revealed a two-fold excess relative to wild type and we found no evidence of changes in the number of apoptotic cells. Pharmacological inhibition of Hh signaling using cyclopamine produced similar effects and also revealed that Hh is required as late as 33 hpf, well after formation of the cerebellar anlage, to limit the number of *olig2*[+] PNs. Although we were unable to investigate formation of eurydendroid cells, because mutant and cyclopamine-treated larvae die before expression of Calretinin, the ventral expansion of *olig2* expression is strongly consistent with a role for DV pattern formation in the cerebellum by Hh signaling.

Wnt signaling is necessary for olig2[+] *PN development*

Similar to ventral neural tube, patterning of dorsal neural tube also depends on secreted factors (Lee and Jessell, 1999; Liem et al., 1995). In particular, *Wnt1* and *Wnt3a* are expressed throughout nearly the entire AP extent of the dorsal CNS (Parr et al., 1993). Mouse *Wnt1* mutants had greatly reduced or nearly absent cerebellums (Bally-Cuif et al., 1995; Thomas and Capecchi, 1990), precluding investigation of cerebellar DV patterning, but *Wnt1/Wnt3a*

double mutants had a deficit of dorsal spinal cord interneurons (Ikeya et al., 1997; Muroyama et al., 2002). Zebrafish *wnt1* and *wnt3l* are expressed prominently in the midbrain at the boundary with hindbrain (Buckles et al., 2004), similar to mouse *Wnt1* and *Wnt3*. Additionally, we detected a lower level of *wnt1* transcripts in dorsal cerebellum at 30 hpf but not 48 hpf, which temporally coincides with Hh-dependent patterning of *olig2*[+] PNs. Notably, the midbrain-hindbrain boundary appeared present in embryos homozygous for a chromosomal deletion spanning *lef1*, which encodes a transcription factor that mediates Wnt signaling. This is a milder phenotype than that produced by *Wnt1* mutation in mice or simultaneous disruption of *wnt1, wnt3l and wnt10b* functions in zebrafish (Buckles et al., 2004). *olig2* expression was entirely absent from the cerebellums of *lef1* deficient embryos, suggesting that Wnt signals are required for PN development. To test this further without the complications of eliminating multiple genes within the chromosomal deficiency or disruption of an early developmental role of Wnt signaling in forming the cerebellar anlage, we induced expression of Dkk1, a Wnt inhibitor, at 30 hpf. Similar to *lef1* deficient embryos, Dkk1 expression blocked *olig2* expression within cerebellum but not in ventral diencephelon or spinal cord. Thus, our data provide evidence that Wnt signaling is necessary for specification of PNs in dorsal spinal cord.

The complementary effects of loss of Hh and Wnt signaling on PN formation suggested that they act in opposition to regulate the number and distribution of PNs. Consistent with this, *wnt1* expression was expanded ventrally in CA-treated embryos and *ptc1* expression, which serves as an indicator of Hh

signaling activity, was expanded dorsally in *lef1* deficient embryos. Additionally, embryos deficient for both Hh and Wnt signaling were identical to embryos that lacked only Wnt signaling in that neither had cerebellar *olig2* expression. We propose that Hh activity limits PN formation by restricting the ventral extent of Wnt signaling, which is necessary for PN specification.

Pattern formation via antagonistic signaling between the Hh and Wnt pathways is an established development mechanism. For example, in the ventral spinal cord Wnt inhibitors regulate transcription of Hh-responsive genes (Lei et al., 2006) whereas in dorsal spinal cord Gli3 repressor inhibits Wnt signaling (Ulloa et al., 2007). Within the epithelium of the colon, high levels of Wnt signaling are restricted to the base of the proliferative crypt by Indian Hedgehog (Ihh), expressed by mature colonocytes, and Ihh reciprocally inhibits expression of Wnt target genes (van den Brink et al., 2004). Our data indicate that antagonistic Hh and Wnt signaling also pattern the DV axis of the zebrafish cerebellum.

CHAPTER III

A GENETIC SCREEN IDENTIFIES A MUTANT DEFECTIVE IN PURKINJE NEURON DEVELOPMENT

Introduction

The cerebellum is a structure critical for balance, motor control and cognition (Holmes, 1939). The neuronal circuitry of the cerebellum is a very elaborate system of afferent and efferent connections that all work together to receive signals from the body, process those signals and relay them back to the body, informing it how to respond. Its organization consists of three layers with one layer, the Purkinje layer, containing only the cell bodies of PNs. PN cell bodies are organized in a monolayer sandwiched between the granule layer, located ventrally, and the molecular layer, located dorsally. The granule layer is comprised of granule neurons whereas the molecular layer contains parallel fibers, stellate, basket and golgi cells. The PN, discovered in 1837 by Johannes Evangelists Purkinje, has a unique structure. Found only within the cerebellum, it has an extensive dendritic arbor and a single opposing axonal projection. PNs receive excitatory input and make inhibitory projections to deep cerebellar nuclei which serve as the sole output from the cerebellum to the cerebellar cortex. Consequently, loss of PNs correlates with ataxia, tremors, abnormal postures and gaits as well as general loss of motor function abilities.

Multiple human diseases such as Freidreich ataxia, Niemann Pick Disease and ataxia telangiectasia all involve rapid degeneration of PNs, which in

turn causes a severe loss of other cell types within the cerebellum (Lechtenberg, 1993; Rotman and Shiloh, 1997). Most of these diseases have early onset during childhood with often fatal results. Identifying the reasons that PNs degenerate and cause overall loss of neurons within the cerebellum is essential to elucidating methods to treat these diseases. Several mouse mutants exist in which degeneration of PNs cause loss of coordination and movement. The *purkinje cell degeneration* (*pcd*) mutant is characterized by a rapid loss of almost all PNs within 45 days after birth, with only 0.5% of PNs surviving to day 30 (Landis and Mullen, 1978; Mullen et al., 1976; Wassef et al., 1986). Degeneration of granule cells, deep cerebellar nuclei and inferior olivary neurons occurs as a secondary effect from loss of PNs, resulting in a 50% reduction in the overall size and weight of the cerebellum (Baurle and Grusser-Cornehls, 1997; Chang and Ghetti, 1993; Triarhou, 1998). However, the gene and mechanism initiating degeneration of PNs occurs has yet to be determined (Wang and Morgan, 2007). Mice deficient in either the *npc1* or *npc2* genes serve as models for the human Niemann-Pick type C disease, an autosomal recessive lipid trafficking disorder (Futerman and van Meer, 2004; Loftus et al., 1997; Ribeiro et al., 2001). The Npc1 protein is a lysosomal protein containing a "sterol sensing domain," which can regulate cholesterol metabolism and has also been shown to interact with the Hh receptor, Ptc (Carstea et al., 1997; Davies et al., 2000; Friedland et al., 2003; Ko et al., 2005; Miyawaki et al., 1982). In the homozygous *npc1* knock out mouse, PNs degenerate in an anterior to posterior manner beginning 30 d after birth (Higashi et al., 1993), and continue to degenerate until only a few PNs exist

in the most posterior lobule (Higashi et al., 1993). Unlike the *pcd* mutant, granule neurons and Bergmann glia, a glial cell that ensheaths the dendritic branches of PNs, are not affected in the *npc1* mutant (Ko et al., 2005). Neither mutant has given many clues as to why PNs begin to undergo cell death or more importantly, how to stop this process from occurring.

In zebrafish, *olig2*, which encodes a bHLH transcription factor, identifies oligodendrocytes, a myelinating cell located within the CNS, as well as a subset of PNs. Previously, we described a transgenic line in which *olig2* regulatory DNA drives expression of EGFP, recapitulating endogenous *olig2* expression (Shin et al., 2003). We utilized this line to perform an ENU mutagenesis screen to identify embryos with a disruption in *olig2*$^+$ PNs. Our screen revealed a mutant that is deficient in the normal number of *olig2*$^+$ PNs. The morphology of the cerebellum suggests overall development of the cerebellum is not severely disrupted. However, a different subset of PNs identified with the anitbody Zebrin II, also show a decrease in number. Other cell types within the cerebellum such as eurydendroid neurons, are still present, although disorganized. These data imply that this mutant, known as *vu225*, has defects in normal PN development and may potentially serve as a model to study PN degeneration in a simple vertebrate system.

Materials and Methods

Zebrafish staging and strains

Pair wise matings produced embryos which were raised at 28.5°C, then staged according to hpf and dpf in addition to morphological criteria (Kimmel et al., 1995). We utilize the transgenic allele *Tg(olig2:egfp)^{vu12}* (Shin et al., 2003) to screen for PN defects. The mutant from the *N*-nitroso-*N*-ethylurea (ENU) screen is identified as Vanderbilt University 225 (*vu225*).

ENU mutagenesis and screening

Male zebrafish of the AB strain were treated according to standard procedure as outlined in Solnica-Krezel et al., to introduce mutations into the male premeiotic germ cells (Solnica-Krezel et al., 1994). These males were then outcrossed to "*Tg(olig2:egfp)^{vu12}*" females to introduce mutations into the F1 generation. F1 progeny were allowed to reach sexual maturation and then crossed to *Tg(olig2:egfp)^{vu12}* fish to produce the F2 families. Progeny from the F2 generation was allowed to mature and were then intercrossed to produce F3 larvae for screening purposes (Figure 3.1). Screening involved observation of 3 dpf- 5 dpf *Tg(olig2:egfp)^{vu12}* F3 embryos to identify phenotypes in which *olig2* expression was altered within the cerebellum. F2 parents were isolated if larvae had misexpression. They were then re-crossed and screened at 24 hpf and 48 hpf to identify embryos with misexpression in the cerebellum but with a properly
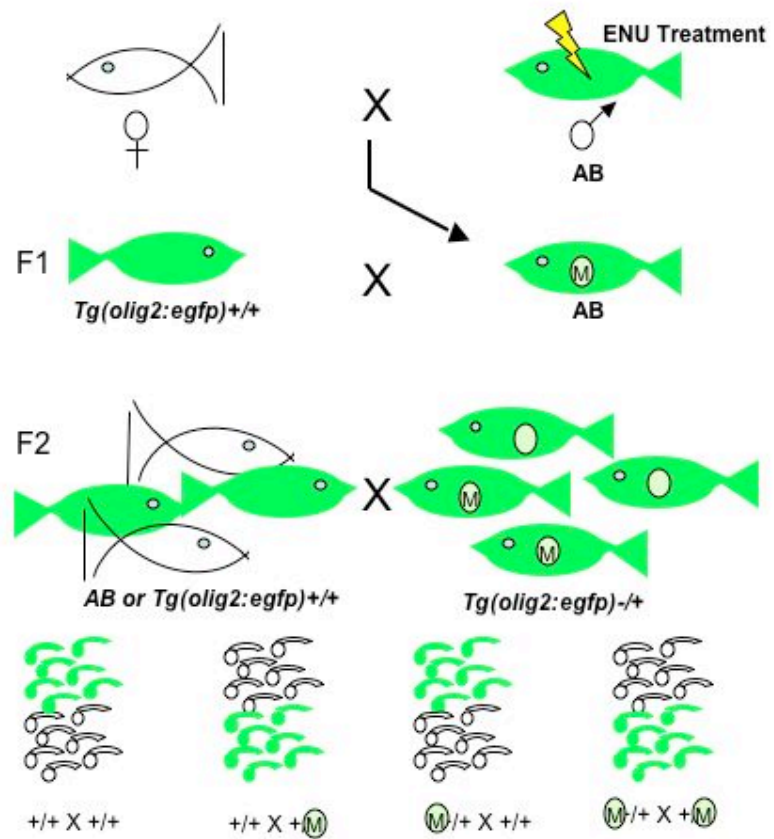
Figure 3.1. Schematic of ENU mutagenesis crosses.

formed cerebellar anlage. Roughly 300 families have been screened and *vu225* is the only cerebellar mutant that has been identified with a fairly normal formation of the cerebellar anlage, misexpression of EGFP in the cerebellum and normal EGFP expression throughout the rest of the embryo.

Immunohistochemistry

The following primary antibodies were used for immunohistochemistry on fixed embryos: rabbit anti-calretinin (1:1000, Swant Products) (Schwaller et al., 1993) mouse anti-parvalbumin (1:1000, Chemicon International) and mouse anti-Zebrin II (1:1000, gift of Dr. R Hawkes) (Brochu et al., 1990). For fluorescent detection we used Alexa Fluor 568 goat anti-mouse conjugate and Alexa Fluor 647 goat anti-rabbit (1:200, Molecular Probes). Embryos intended for sectioning were embedded in 1.5% agar/5% sucrose and frozen by immersion in liquid nitrogen while in 2-methyl-butane. Whole mount fluorescent images were collected using a QImaging Retiga Exi color CCD camera mounted on an Olympus AX70 compound microscope and imported into Adobe Photoshop. For sectioned embryos, a cryostat microtome was used to obtain tissues of 10 µm thickness. Fluorescent images of sectioned embryos were collected using a 40X oil-immersion (NA = 1.3) objective mounted on a motorized Zeiss Axiovert 200 microscope equipped with a PerkinElmer ERS spinning disk confocal system or a Zeiss LSM510 Meta laser scanning confocal microscope and imported into Volocity (Improvision). All image manipulations were restricted to adjustment of levels, curves, saturation and hue.

Whole mount imaging

Embryos for whole mount visualization were treated with MESAB (3-amino-benzoic acid ethyl ester) and placed in 1.5% methyl cellulose for live imaging. Whole mount fluorescent and DIC images were collected using a QImaging Retiga Exi color CCD camera mounted on an Olympus AX70 compound microscope and were collected using Openlab (Improvision) software and exported to Adobe Photoshop. All image manipulations were restricted to adjustment of levels and hues.

Results

Genetic screen for mutations that disrupt formation of olig2$^+$ PNs

To discover mutations in genes with essential functions in formation and specification of *olig2$^+$* PNs, we conducted a screen for zebrafish mutants with disrupted cerebellar EGFP expression in *Tg(olig2:egfp)^{vu12}* embryos. This screen was performed in conjunction with a screen for disruption of oligodendrocytes, the myelinating cell within the CNS, which also express *olig2* and are identified by their dorsal position in the spinal cord in *Tg(olig2:egfp)^{vu12}* embryos. To screen through as many families as possible close examination of F3 embryos did not begin until 3 dpf. At this time point the oligodendrocytes have migrated to their dorsal position, making it easy to screen for disruptions in number and position within the spinal cord. Expression of *olig2* transcript in the cerebellum is evident around 36 hpf by in situ RNA hybridization, however EGFP expression is evident

by 40 hpf. By 3 dpf *olig2*$^+$ PNs in the cerebellum have extended their ventral

axonal projections close to the midbrain-hindbrain (MBHB) boundary and have

begun initial dendritic branching, thus making it easy to detect at 3 dpf if there are

disruptions in *olig2*$^+$ PNs. Initially, many cerebellar mutants were identified,

mainly for a complete lack of any *olig2*$^+$ PNs in the cerebellum. However, closer

examination of these mutants revealed the reason for the lack of *olig2*$^+$ PNs was

there was no cerebellum.

Previous studies have already identified multiple mutations in genes

resulting in the loss of the cerebellar structure, such as *acerebellar* (*ace*), *no*

isthmus (*noi*) and *spiel ohne grenzen* (*spg*), all resulting in mutations in genes

important for proper formation of the MBHB boundary (Belting et al., 2001; Brand

et al., 1996). To avoid identifying more MBHB mutants, embryos lacking a

cerebellum did not become our main focus, instead we looked specifically at

mutants with disruption in *olig2*$^+$ PNs with a morphologically present cerebellum.

These criteria limited our findings to a single mutant, *vu225*.

Phenotypic characterization of vu225

To characterize the phenotype of *vu225* we crossed F2 identified *vu225*

carrier *Tg(olig2:egfp)*^{vu12} adults to analyze overall morphology beginning at 48

hpf. By 48 hpf the cerebellar anlage is visible as well as portions of the fourth

ventricle in both the WT and *vu225* mutant. A dorsal view of the mutant reveals a

clearly formed cerebellar anlage (Figure 3.2 K). The overall length of *vu225*

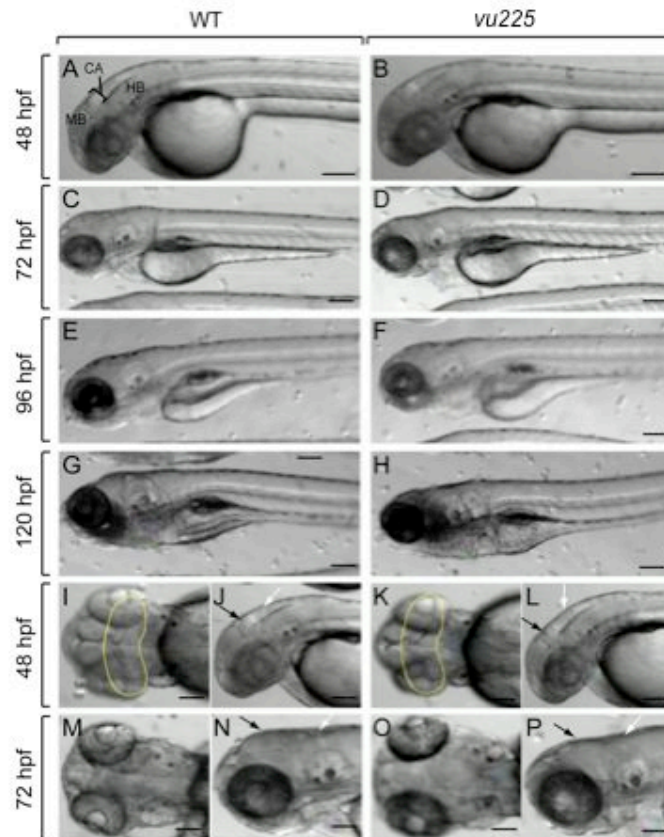mutant embryos is slightly shorter than WT but the head is relatively normal. The

65

Figure 3.2. *DIC images of WT compared to vu225 mutant embryos show morphological presence of cerebellum, flattened head and missing inflated swim bladder.* All panels are whole mount images with anterior to the left. Black arrows depict cerebellum, yellow circles outline cerebellum in dorsal views. Midbrain (MB), Cerebellum Anlage (CA), Hindbrain (HB) are marked. (A,C,E,G) Developmental time course depicting WT formation of the cerebellar anlage by 48 hpf and a swim bladder by 120 hpf. (I,J,M,N) Dorsal and sagital views illustrating closer view of cerebellum. (B,D,F,H) Sagital views of *vu225* mutant embryos showing formation of cerebellar anlage at 48 hpf and a lack of a swim bladder by 120 hpf. (K,L,O,P) Dorsal and sagital views of the mutant cerebellum clearly showing properly formed cerebellum. Scale bars represent 20 μm in all panels.

fourth ventricle in some embryos is somewhat enlarged compared to the WT

ventricle. This is most likely due to some potential defect or delay in the closure

of the fourth ventricle, not an increase in its size (Figure 3.2 A, B, I-L). In addition

to these phenotypes some mutants have a slightly curved trunk, but properly

formed somites. At 72 hpf the cerebellum in WT embryos is no longer readily

distinguishable and the fourth ventricle is no longer visible. However, in *vu225*

mutant embryos the head is smaller and flattened on the dorsal region of the

midbrain. Importantly, there is no grey tissue often implicating necrosis (Figure

3.2 C, D, M-P). At 96 and 120 hpf the overall morphology of the *vu225* mutant is

similar to the WT embryo. The jaw protrudes normally, however the head is

smaller and remains flattened across the midbrain region (Figure 3.2 E-H). At

120 hpf WT embryos inflate a swim bladder, however *vu225* mutant embryos do

fail to do so and as they reach 144 hpf and beyond they begin to develop severe

cardiac edema and die between 144-168 hpf.

Analysis of EGFP expression in the vu225 cerebellum

Cerebellar EGFP expression in *vu225* has a very obvious phenotype. At

48 hpf two severities of EGFP expression deficiency can be identified in the

cerebellum. One class of *vu225* mutant embryos show no cerebellar expression.

Whereas others maintain some EGFP expression, however, it is reduced in

comparison to WT embryos (Figure 3.3 A, B). In the *vu225* mutant embryos that

do show EGFP expression in the cerebellum, expression does not extend

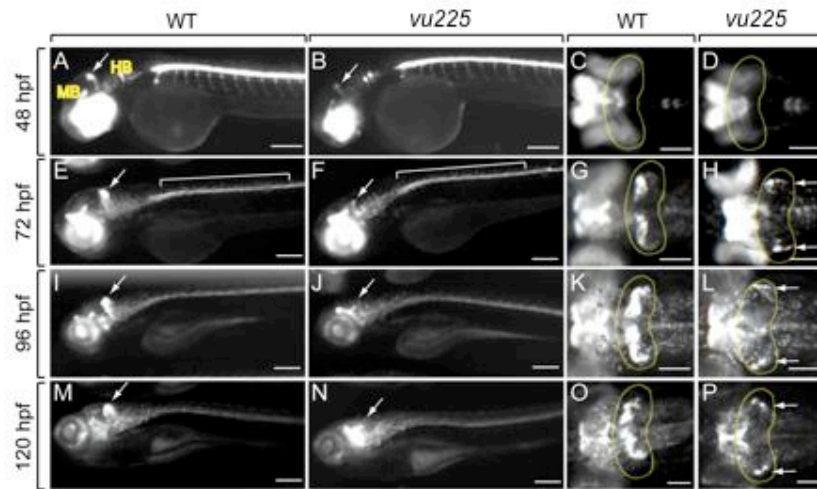dorsally to the extent it does in WT and there seems to be fewer EGFP$^+$ cells

Figure 3.3. *A developmental time course comparison of EGFP expression in Tg(olig2:egfp) WT embryos and vu225 mutants reveal the complete absence or severe decrease in EGFP⁺ cells within the cerebellum.* All panels are whole mount images with anterior to the left. White arrows depict EGFP⁺ cells within the cerebellum, yellow circles outline cerebellum in dorsal views. Midbrain (MB) and Hindbrain (HB) are marked. (A,C,E,G,I,K,M,O) Developmental time course depicting WT EGFP in live *Tg(olig2:egfp)* embryos in either lateral or dorsal views starting at 48 hpf up to 120 hpf where EGFP expression is becoming increasingly robust. (B,D,F,H,J,L,N,P) Developmental time course depicting EGFP expression in live *vu225;Tg(olig2:egfp)* embryos in either lateral or dorsal views starting at 48 hpf up to 120 hpf in which EGFP expression within the cerebellum is dramatically decreased or absent while EGFP expression throughout the remainder of the embryo is like WT. Scale bars represent 20 μm in all panels.

present overall. In the spinal cord, however, EGFP expression is maintained and looks identical to WT expression in both phenotypes. At this stage a dorsal view of *vu225* mutant embryos reveal a relatively normal looking cerebellum, however EGFP expression indicates there are no EGFP$^+$ cells approaching the midline of the cerebellum (Figure 3.3 C, D). By 72 hpf there seems to be a reduction in EGFP$^+$ cells in the cerebellum compared to EGFP expression just 24 hours prior in the mutant (Figure 3.3 E-F). Mutant EGFP$^+$ cells in the spinal cord have migrated to their normal dorsal position similarly to WT embryos (Figure 3.3 E-F). At 72 hpf a dorsal view of the mutant embryos reveals a very noticeable decrease in EGFP$^+$ cells in the cerebellum as well as a complete lack of EGFP$^+$ cells to extend to the midline of the cerebellum (Figure 3.3 G, H). Mutant embryos at 96 hpf seem to either maintain or possibly even lose more EGFP$^+$ cells in the cerebellum (Figure 3.3 I-L). A dorsal view at 120 hpf depicts very laterally placed EGFP$^+$ cells in the cerebellum, unlike the WT embryos, which exhibit robust EGFP expression broadly across the cerebellum (Figure 3.3 O-P). Interestingly, the EGFP expression in the spinal cord, forebrain and hindbrain in *vu225* mutant embryos is not disrupted.

Specification of cerebellar cell types in vu225 mutant

To determine if *vu225* affects only *olig2*$^+$ PNs, we examined other cerebellar cell types. Immunohistochemistry with the antibody Calretinin identifies eurydendroid neurons in the zebrafish cerebellum. PNs either project ventrally onto eurydendroid neurons or continue to project past them (Refer to Figure 2.2

I, J). To determine if eurydendroid neurons are present in *vu225* mutants embryos were fixed at 120 hpf and immunohistochemistry was performed on transverse sections through the cerebellum of *Tg(olig2:egfp)* embryos. In WT embryos, cerebellar EGFP$^+$ PNs are evenly distributed from the most lateral/ventral portion of the cerebellum and stay along the outer ridge of the cerebellum up to the midline/dorsal region (Figure 3.4 A). Calretinin$^+$ eurydendroid neurons follow along this same path directly underneath the EGFP$^+$ cells (Figure 3.4 A', A"). In a transverse section of *vu225* we can clearly see the lateral/ventral positioning of EGFP$^+$ cells in the cerebellum, however they do not extend up to the dorsal/midline region of the cerebellum (Figure 3.4 B). In contrast to WT embryos, only a small number of Calretinin$^+$ cells gather directly underneath the EGFP$^+$ cells, instead they are scattered throughout the medulla oblongata region (Figure 3.4 B', B").

Previously we have identified two distinct subsets of PNs, EGFP$^+$ and Zebrin II$^+$(Refer to Figure 2.2 G, H, J). To determine if the mutation in *vu225* disrupted all PN development or specifically EGFP$^+$ PNs, we analyzed Zebrin II expression in 120 hpf transverse cerebellar sections. Zebrin II$^+$ PNs in WT embryos are intermixed and slightly dorsal to EGFP$^+$ PNs (Figure 3.5 A-A'''). However, *vu225* mutants have a decreased number of Zebrin II$^+$ cells and are only present when there are EGFP$^+$ PNs present in the ventral/lateral domain (Figure 3.5 B-B'''). These data show that other PNs are present and can be specified, however the number of both *EGFP*$^+$ and Zebrin II$^+$ PNs is dramatically smaller than that of WT.
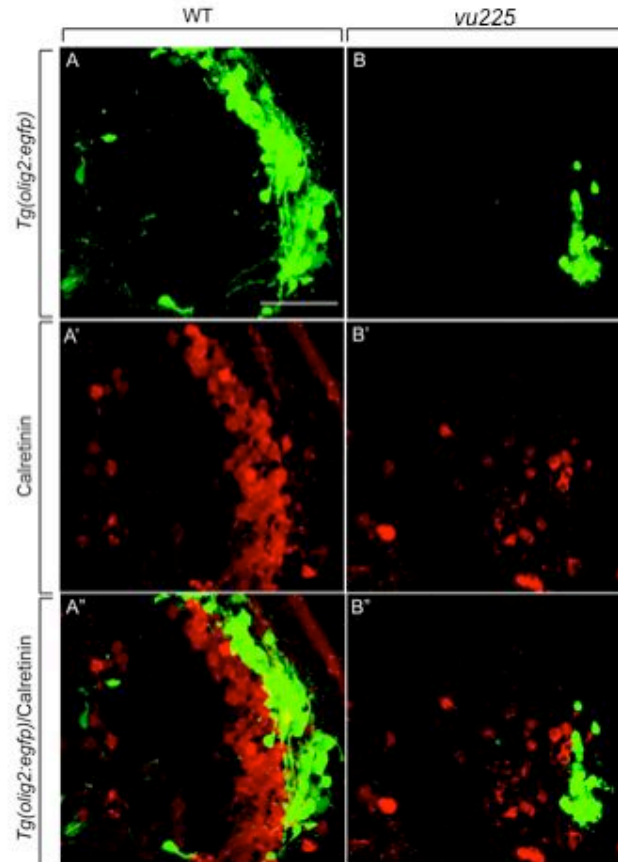
Figure 3.4. *Transverse sections of Tg(olig2:egfp) embryos through the cerebellum reveal improperly positioned and a general decrease in EGFP⁺ and Calretinin⁺ cells in vu225 when compared to WT.* (A-A‴) *Tg(olig2:egfp)* embryos with Calretinin antibody shows DV organization of EGFP⁺ and Calretinin⁺ cells. (B-B‴) *vu225 Tg(olig2:egfp)* embryos show a decrease in Calretinin⁺ and EGFP⁺ cells. Scale bars represent 10 µm in all panels.
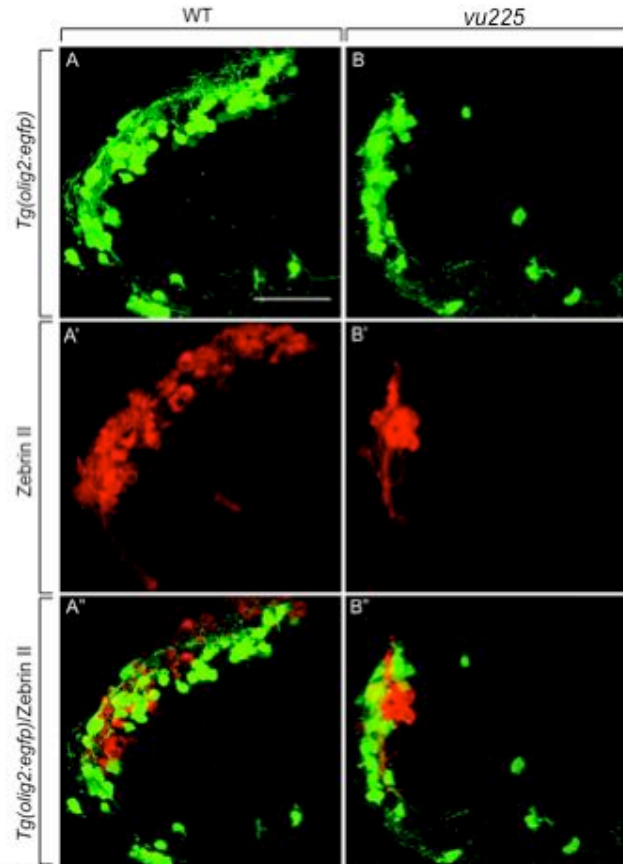
Figure 3.5. *Transverse sections of Tg(olig2:egfp) embryos through the cerebellum reveal a decrease in EGFP+ and Zebrin II+ PNs.* (A-A″) *Tg(olig2:egfp)* embryos with Zerbin II antibody shows distinct populations of PNs intermixed within the PN layer. (B-B″) *vu225 Tg(olig2:egfp)* embryos show very little Zebrin II+ PNs but are present only with EGFP+ PNs when they are present. Scale bars represent 10 μm in all panels.

To be certain we identified all PNs, we utilized Parvalbumin (PV), an antibody used to identify PNs. PV is a Calcium binding Protein (CaBP) belonging to the EF-hand family of proteins (Celio, 1990). PV has been shown to label PNs in mammalian systems as well as PNs in other adult teleosts, however no published work has determined its expression in a zebrafish embryo (Alonso et al., 1992; Crespo et al., 1999; Schmidt et al., 2007). In mammals another CaBP termed Calbindin is most often associated with identifying PNs. However, in teleosts the homolog to Calbindin is Calretinin, which we have already shown to alternatively label eurydendroid neurons. In the WT 120 hpf transverse sections PV does not colabel with EGFP$^+$ PNs, however there are PV$^+$ cells intermixed within the EGFP $^+$ PN layer. It also appears that there is a distinct pattern that forms with the PV$^+$ cells. They are found almost exclusively towards the midline/dorsal region of the cerebellum with very few located along the lateral or lateral/ventral domain (Figure 3.6 A-A'''). In the *vu225* mutant PV$^+$ cells display a similar pattern to Zebrin II$^+$ PNs and are located only where EGFP $^+$ PNs are present along the ventral/lateral domain (Figure 3.6 B-B'''). These data also support that in the *vu225* mutant all PN populations are somehow affected although still able to be specified. A schematic depicting the organization of PNs in the WT embryo and how their patterns are altered in the *vu225* mutant are summarized in Figure 3.7.
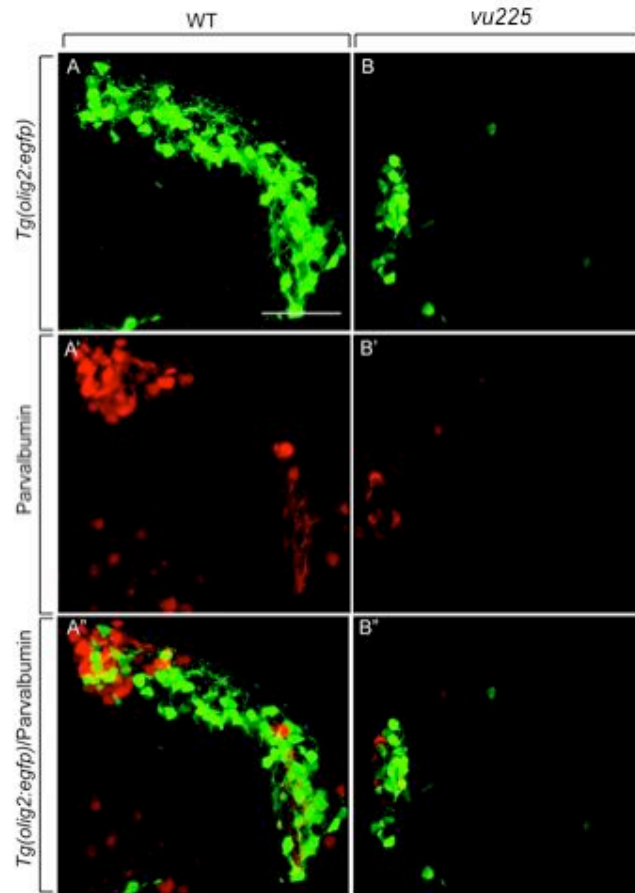
Figure 3.6. *Transverse sections of Tg(olig2:egfp) embryos through the cerebellum reveal a decrease in EGFP⁺ and PV⁺ PNs. (A-A")* Tg(olig2:egfp) embryos with PV antibody shows distinct population of PNs intermixed within the PN layer. (B-B") *vu225 Tg(olig2:egfp)* embryos show very little PV⁺ PNs but are present only with EGFP⁺ PNs when they are present. Scale bars represent 10 µm in all panels.

D/M

L/V

WT

D/M

L/V

vu225

■ Zebrin II⁺ PNs

■ *olig2*⁺ PNs

■ Calretinin⁺ Eurydendroid neurons
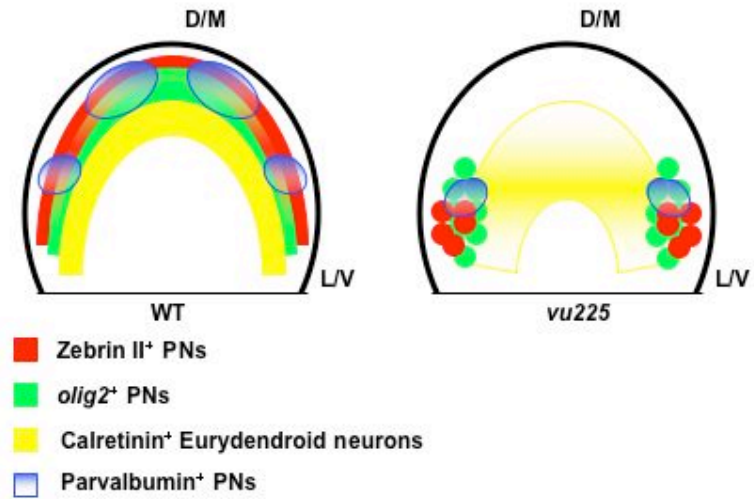
□ Parvalbumin⁺ PNs

Figure 3.7. *Model of a transverse section through the cerebellum depicting WT cerebellar cell type expression versus vu225. Dorsal/Medial (D/M) and Lateral/Ventral (L/V). Note although we have evidence supporting olig2⁺ and PV⁺ PNs are distinct subsets, we do not know if this is the same for Zebrin II⁺ and PV⁺ PNs.*

Discussion

Cerebellar specific mutation

 Our ENU screen has produced many interesting mutants however, only one mutant has demonstrated a clear cerebellar specific phenotype. To identify a mutant with very little or no EGFP^{+} cells in the cerebellum, but still form a cerebellum, is ideal for identifying cerebellar specific mutations. Our data determining cell specification in the *vu225* mutant also indicate that this mutation potentially only has severe effects on the PN population. Calretinin^{+} cells are present although they did not have their normal number or distribution. This is most likely due to the fact that there are very few PNs present. These data may indicate that PNs are necessary to properly pattern eurydendroid neurons in the zebrafish cerebellum. This would be a logical finding since PNs are known to project onto and past eurydendroid neurons. If there are no PNs present to receive contact or input from, they may not be receiving signals informing them of their proper position. However a more detailed analysis quantifying the number of eurydendroid neurons present is needed as well as a more thorough examination of other cerebellar cells types before this conclusion can be made.

Behavioral defects in vu225

 Because the cerebellum is the control center for balance and coordinated movement, there is a good chance the *vu225* mutants would exhibit a lack of coordination while swimming. Previously, we noted that some *vu225* mutants

also exhibited a slightly curvy tail phenotype. When gently prodded with the tip of a forcep these embryos either had no reaction or tried briefly to swim away which resulted in spinning in the same spot. This is most likely due to the malformed tail and so these embryos were disregarded for any behavioral observation (data not shown). 5 dpf larvae lacking a curvy tail as well as EGFP expression in the cerebellum were prodded with the forcep and observed for their coordination ability. Surprisingly, they were able to swim away from the forcep. However, whereas it took a WT embryo one or two touches at most to react, the *vu225* could take as many as twelve touches to react to the forcep (data not shown). Interestingly, when the WT embryos are prodded they often swim out of view from the microscope. By contrast, when the *vu225* mutants did respond to touch they did not swim far and remained within the field of view.

Our data taken together indicate our screen has caused a mutation in a gene or multiple genes that effect normal cerebellar development. This most likely occurs by causing defects in PN development as shown by EGFP, Zebrin II and PV expression in the cerebellum. This mutant may also provide good insight as to the importance of PN development in properly patterning other cerebellar cells. Previous studies have shown in the mouse mutants such as Scrambler, Meander tail and Reeler that the cytoarchitecture of the cerebellum is often disrupted with ectopic PNs and lack of or mispatterned granule neurons. However identifying how misplacement of granule neurons or PNs affects other cell types is not fully understood. The *vu225* mutant may provide some insight as to how this occurs and how it may specifically effect PNs.

Future Directions

In order to characterize the *vu225* mutant as thouroughly as possible in situ RNA hybridization will be carried out for *atoh1a*, a marker for granule neurons within the rhombic lip, which can help determine the actual formation of the cerebellum. Other neuronal markers such as *zash1a*, *neurogenin*, and *zic1* can also be used to identify multiple cell types within the cerebellum. Comparison to WT embryos would determine if any of these expression patterns are disturbed. In addition, live imaging would be necessary for both cell counts and tracking the *olig2*[+] PNs in time lapse imaging to determine if there is indeed a degeneration of PNs. Analysis of cell death in the *vu225* mutant would also give an indication if multiple cell types are undergoing cell death or if it is limited to PNs.

In addition to fully characterizing the *vu225* mutant phenotype, genetic mapping analysis using PCR based polymorphic markers would be used to determine the actual gene or genes that are mutated, responsible for the mutant. DNA from multiple *vu225* mutant embryos will be pooled for bulk segregant analysis and compared to WT DNA for markers along multiple points along the 25 zebrafish chromosomes. After a region has been narrowed down several more markers will be needed to further pinpoint the area of interest and hopefully eventually lead to the identification of the gene or genes that are disrupted.

Acknowledgements

CHAPTER IV

TREATMENT WITH A BMP ANTAGONIST PRODUCES EXCESS DORSALLY LOCATED OLIGODENDROCYTES IN THE ZEBRAFISH SPINAL CORD

Introduction

Myelin is an essential component throughout the vertebrate nervous system, which facilitates rapid salutatory conduction along axons. Myelin is produced by only one cell type within the central nervous system (CNS), oligodendrocytes. These oligodendrocytes can have multiple processes from a single cell body that will wrap numerous axons. They wrap axons in highly compacted concentric myelin sheaths, leaving a small area of axon unprotected, termed the node of Ranvier, that contains the voltage-gated sodium channels responsible for the rapid transmission of action potentials to the next node of Ranvier. Human diseases such as Multiple Sclerosis (MS) are often associated with degeneration of these myelin sheaths and the inability of oligodendrocytes to properly remyelinate the exposed axons. Although much work has been done to understand the signals necessary to promote specification of oligodendrocytes from their established site of origin, the pMN domain, recent work has focused on signals that prohibit oligodendrocyte differentiation. Understanding the signals regulating oligodendrocyte differentiation may lead to novel methods of inducing oligodendrocyte differentiation in areas that may lead to remyelination after an injury to the myelin sheath.

A gradient of Shh expressed from the notochord induces transcription of *olig2*, one of the earliest factors regulating oligodendrocyte specification (Lu et al., 2000; Park et al., 2004; Zhou et al., 2000). Oligodendrocyte progenitor cells (OPCs) express *olig2* while in the ventral pMN domain and express Sox10 when they begin migration to dorsal and ventral locations where they will begin to wrap axons (Stolt et al., 2002). Shh is both necessary and sufficient to induce oligodendrocytes both in vitro and in vivo. Grafting experiments and cultured explants have also shown that Shh can induce oligodendrocyte formation in the dorsal spinal cord (Orentas and Miller, 1996; Poncet et al., 1996; Pringle et al., 1996). These data indicate that dorsal neuroepithelium has the capacity to produce oligodendrocytes but cannot, possibly due to factors inhibiting their differentiation. Recent work has also shown that oligodendrogenesis can occur in the dorsal spinal cord in the absence of Hh signaling (Cai et al., 2005), indicating other signals may be involved in specification of oligodendrocytes. Evidence to support the idea of a dorsal inhibitory factor playing a role in oligodendrocyte specification originally came from cultured spinal cord cells. When ventral and dorsal spinal cords were cultured separately there was a robust increase in the number of oligodendrocytes within the ventral portion of the spinal cord (Wada et al., 2000). In addition, experiments that ablated the dorsal most portion of the spinal cord produced an increase in oligodendrocytes (Mekki-Dauriac et al., 2002). These data are indicative that dorsally secreted signals are inhibiting the differentiation of mature oligodendrocytes.

Current theories for DV patterning within the spinal cord have been extensively described and have established ventral and dorsal antagonistic gradients of secreted proteins are necessary for proper differentiation of cell types along the DV axis (Jessell, 2000; Lee et al., 2000; Tanabe and Jessell, 1996). Shh is secreted from the ventral notochord, thus providing the ventral gradient, and BMPs are expressed from the dorsal roof plate creating a dorsal to ventral gradient that antagonizes the Shh gradient (Liem et al., 2000; Liem et al., 1995). BMP antagonists such as noggin and chordin are expressed from the notochord and floor plate (Tanabe and Jessell, 1996) and work from Mekki-Dauriac has shown with grafts of noggin producing cells that differentiation of oligodendrocytes can occur in the presence of a BMP antagonist in dorsal regions of the spinal cord where oligodendrocyte differentiation does not normally occur (Mekki-Dauriac et al., 2002). In vitro work has demonstrated that high levels of BMPs can block specification of oligodendrocytes and dorsal spinal cord explants treated with BMP antagonists such as noggin and chordin can induce specification of oligodendrocytes (Piccolo et al., 1996; Vallstedt et al., 2005; Zimmerman et al., 1996). In vivo work examining the role of BMPs in oligodendrocyte specification has been very limited thus far. BMP overexpression studies in the mouse have shown a decrease in mature oligodendrocytes (Gomes et al., 2003), while implantation of beads soaked in anti BMP4- antibody that blocks BMP activation in *Xenopus* dorsal spinal cord, induced formation of ectopic oligodendrocytes (Miller et al., 2004). However, more in vivo work is

necessary to determine the role BMPs play in blocking oligodendrocyte specification.

Our lab has described a zebrafish transgenic line in which *olig2* regulatory DNA drives expression of EGFP, recapitulating endogenous *olig2* expression (Shin et al., 2003). Due to the transparent development of zebrafish, we can use live imaging to record the EGFP $^+$ oligodendrocytes within the spinal cord. Using a novel compound, which blocks BMP signaling termed HY (personal communication with Dr. Charles Hong at Vanderbilt University), we have explored the effect inhibition of BMPs has on the specification of oligodendrocytes within the zebrafish spinal cord. Our findings thus far indicate that there is an increase in dorsally located EGFP $^+$ OPCs when very few are normally present. Immunohistochemistry labeling with anti Sox 10 antibody reveals *sox10*$^+$ OPCs present in the spinal cord at 48 hpf, at least twelve hours before this is normally seen in WT embryos, indicating a possible role for BMPs to inhibit oligodendrocyte specification in the zebrafish spinal cord.

Materials and methods

Zebrafish strains and embryo culture

Adult zebrafish were maintained according to standard procedures as previously described (Kimmel et al., 1995). Embryos were produced by natural matings and raised at 28.5°C in egg water or EM, then staged according to hpf

and dpf in addition to morphological criteria (Kimmel et al., 1995). The stable transgenic line *Tg(olig2:egfp)^{vu12}* (Shin et al., 2003) was used for this study.

Immunohistochemistry

We used rabbit anti-sox 10 (generated by the Appel lab) as the primary antibody for immunohistochemistry. For fluorescent detection we used Alexa Fluor 568 goat anti-rabbit conjugate (1:200, Molecular Probes). All embryos for sectioning were embedded in 1.5% agar/5% sucrose and frozen in 2-methyl-butane chilled by immersion in liquid nitrogen. Sections of 10 µm thickness were obtained using a cryostat microtome. Fluorescent images of sectioned embryos were collected using a 40X oil-immersion (NA = 1.3) objective mounted on a motorized Zeiss Axiovert 200 microscope equipped with a PerkinElmer ERS spinning disk confocal system or a Zeiss LSM510 Meta laser scanning confocal microscope and imported into Volocity (Improvision). Whole mount fluorescent images were collected using a QImaging Retiga Exi color CCD camera mounted on an Olympus AX70 compound microscope and imported into Adobe Photoshop. All image manipulations were restricted to adjustment of levels, curves, saturation and hue.

Results

Treatment with HY compound at 24 hpf results in excess dorsal OPCs

Inhibition of BMPs from very early on in development results in an expansion in dorsal embryonic structures at the expense of ventral structures (Kishimoto et al., 1997; Re'em-Kalma et al., 1995). To study the effects blocking BMPs has on specification of OPCs at later stages of development, HY compound was added to egg water with the embryos, allowing for effective blocking of BMP signaling at later time points so as not to disrupt overall formation of the embryo. To determine the dosage necessary to block BMPs, we started with 10 μM and 20 μM concentrations. Normally, *olig2*$^+$ OPCs do not begin their dorsal migration until around 48 hpf, therefore we added HY compound to *Tg(olig2:egfp)^{vu12}* embryos as early as 10 hpf and as late as 24 hpf and observed at 48 hpf to determine if blocking BMPs disrupted normal oligodendrocyte differentiation.

We observed a dose dependant effect on dorsally located EGFP$^+$ OPCs. At 48 hpf, WT embryos have just begun OPC dorsal migration from the ventral pMN domain (Figure 4.1 A-A'''). Dorsal migration occurs in an anterior to posterior pattern and in WT is restricted to the first 5-6 somites after the hindbrain. In contrast, embryos treated with 10 μM HY compound at 24 hpf display not only an increase in dorsally located OPCs but also a posterior extension in dorsal EGFP$^+$ cells above the pMN domain (Figure 4.1 B-B'''). Treatment with 20 μM of HY shows a more dramatic effect on dorsally located
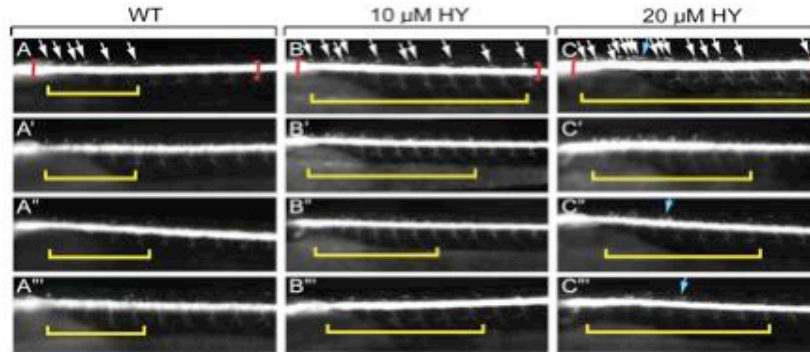
Figure 4.1. *EGFP expression in the spinal cord reveals a dose dependant increase in dorsally located olig2+ OPCs when Tg(olig2:egfp) embryos are treated with HY compound at 24 hpf.* White arrows indicate dorsally located EGFP+ OPCs and blue arrows depict dorsal EGFP+ OPCs with an elongated morphology. Yellow brackets show the area along the AP axis EGFP+ OPCs have migrated dorsally and red brackets depict the EGFP+ ventral portion of the spinal cord. (A-A'") Dorsally migrated EGFP+ OPCs are generally restricted to the dorsal portion of *Tg(olig2:egfp)* embryos. (B-B'") *Tg(olig2:egfp)* embryos treated with 10 μm of HY compound show an increase in the number of dorsally located EGFP+ OPCs and in increase in the number of dorsal EGFP+ OPCs along the AP axis. (C-C'") *Tg(olig2:egfp)* embryos treated with 20 μm of HY compound show an increase in the number of dorsally located EGFP+ OPCs and in increase in the number of dorsal EGFP+ OPCs along the AP axis. Scale bars represent 20 μm in all panels.

EGFP+ cells (Figure 4.1 C-C"'). These embryos also exhibit the posterior

extension of dorsally migrated OPCs, indicating these OPCs are appearing in the

dorsal position much earlier when compared to WT embryos. Usually dorsally

located OPCs have a rounded shape at 48 hpf however, around 3 dpf they begin

to elongate as they find their axons and begin wrapping them with myelin.

Interestingly, in embryos treated with 20 μM HY this elongated morphology can

be seen in several dorsally located EGFP+ OPCs, a full day before they are

observed in WT. These data raise two possibilities, one is that inhibition of BMP

signaling allows for OPCs to migrate dorsally at an earlier time point, or two,

inhibition of BMPs allows for differentiation of OPCs into mature

oligodendrocytes.

Sox 10 labeling indicates HY causes early specification

To investigate the possibility that inhibition of BMPs causes early

differentiation of OPCs we performed immunohistochemistry with a marker to

identify differentiated OPCs. There are three steps OPCs undergo to become a

mature oligodendrocyte. First, they express *olig2* while within the pMN domain,

once they are ready to migrate they express Sox10, indicating they are specified

to become oligodendrocytes. Once they have stopped migrating they will

differentiate and begin to wrap axons and produce myelin, expressing factors

such as *myelin binding protein* (*mbp*). In mammals it has been shown that Sox

10 is necessary for activation of *mbp* through protein-protein interactions

between Sox 10 and Sp1 (Wei et al., 2004).

Transverse sections through the spinal cord of 48 hpf $Tg(olig2:egfp)^{vu12}$ were labeled with Sox 10 antibody. In these WT sections we saw very few dorsally located Sox 10^+ cells and as expected when we did observe a dorsally positioned Sox 10^+ cell, it was always colabeled with $EGFP^+$ (Figure 4.2 A-C). However, in $Tg(olig2:egfp)^{vu12}$ embryos treated with 20 μM of HY, in addition to dorsally located $EGFP^+/Sox 10^+$ colabeled OPCs (data not shown, summarized in Figure 4.3), we also saw a significant increase in Sox 10^+ dorsally positioned OPCs (Figure 4.2 D-L, Figure 4.3). These data indicate that inhibition of BMPs is potentially causing either early specification or early migration of $sox10^+$ OPCs to dorsal positions within the spinal cord.

Blocking BMPs results in improperly positioned oligodendrocytes

To determine if the position of oligodendrocytes is normal even though they seem to differentiate early, we used Sox 10 as a marker and performed immunohistochemistry on 3 dpf $Tg(olig2:egfp)^{vu12}$ embryos. At this stage OPCs have migrated to the outer ridge of the spinal cord in the white matter to begin to wrap axons. A typical transverse section through the spinal cord in a WT embryo will yield one or two $EGFP^+$ dorsally opposing positioned cells colabeled with Sox 10, residing in the white matter (Figure 4.4 D-F). Occasionally, we will find the dorsal OPC's are located on the same side, however this is a somewhat rare occurrence (Figure 4.4 A-C). In $Tg(olig2:egfp)^{vu12}$ embryos treated with 20 μM HY, many of the dorsally located OPCs are positioned within the grey matter, located more medially than the white matter (Figure 4.4 G-I). However, there are
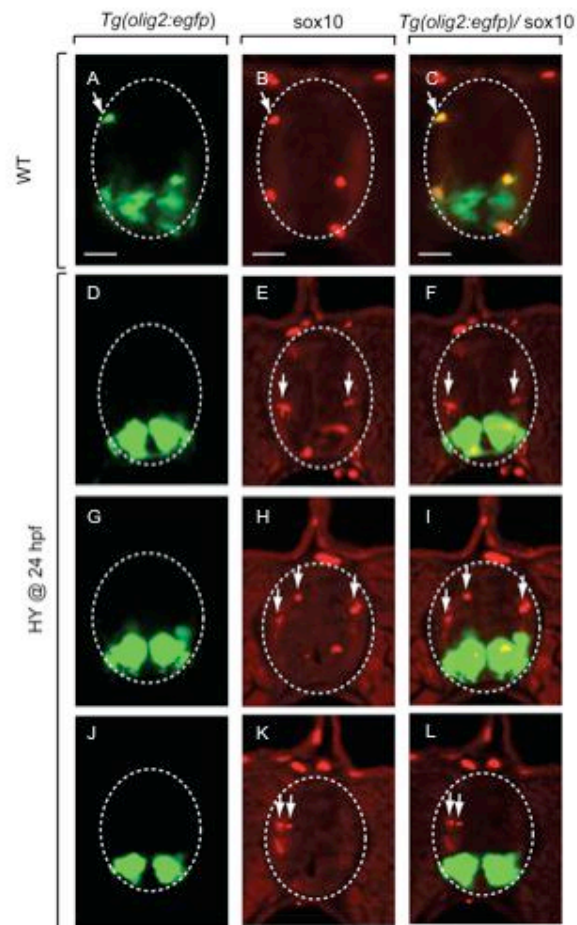
Figure 4.2. *Sox10 antibody labeling reveals sox10⁺;EGFP⁻ dorsally located OPCs at 48 hpf.* Transverse sections through *Tg(olig2:egfp)* embryos. White arrows depict *sox10⁺;EGFP⁻* and *sox10⁺;EGFP⁺* OPCs. (A-C) WT *Tg(olig2:egfp)* embryos labeled with *sox10* antibody show the rarely found *sox10⁺;EGFP⁺* OPC in its normal dorsal location at 48 hpf. (D-L) *sox10* antibody labeling on *Tg(olig2:egfp)* embryos treated with HY at 24 hpf reveal a dramatic increase in dorsally located *sox10⁺;EGFP⁻* OPCs. Scale bars represent 20 μm in all panels.
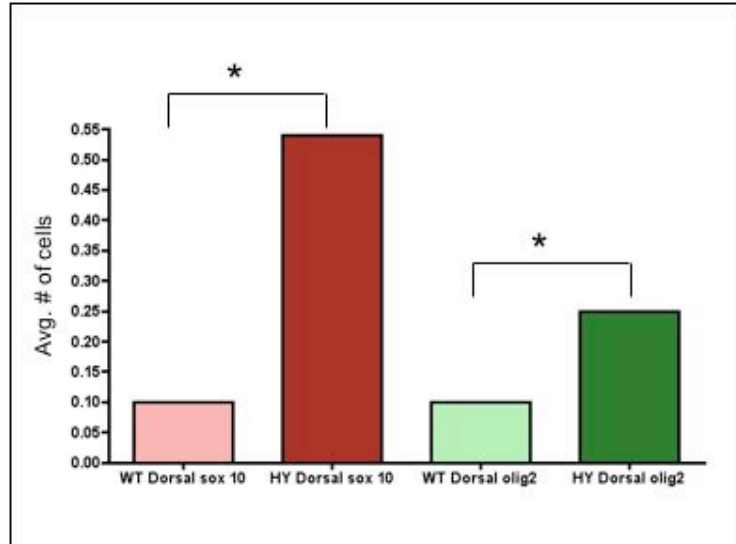
Figure 4.3. *Graph representing the increase in sox10⁺ and EGFP⁺ dorsally located OPCs within the spinal cord at 48 hpf.* ∗ represents significant difference p<0.05 as performed by student t test. n=40 sections for each assay.
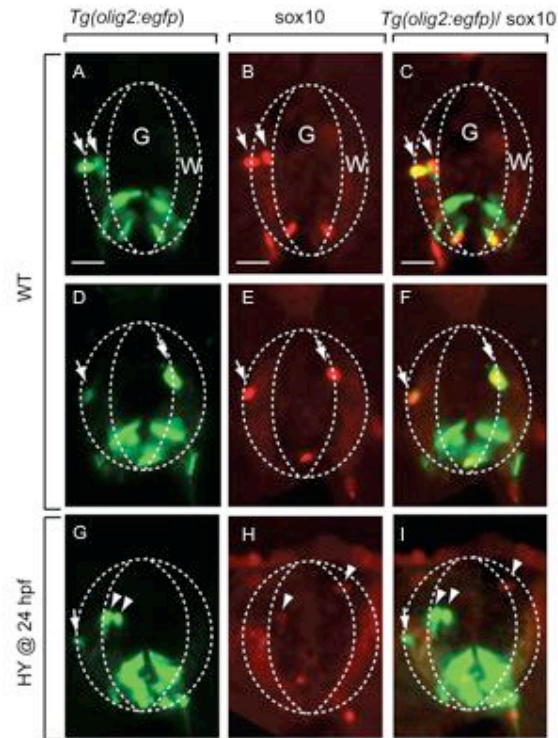
Figure 4.4. *Sox10 antibody labeling reveals an increase of OPCs in the grey matter of embryos treated with HY*, All panels are transverse sections through spinal cord at 72 hpf. White arrows show *EGFP⁺;sox10⁺* positioned within the White matter. White arrow heads illustrate *EGFP⁺;sox10⁺* and *EGFP⁻;sox10⁺* OPCs positioned in the grey matter. Grey matter (G), White matter (W). (A-C) WT *Tg(olig2:egfp)* embryo depicting normal positioning of *EGFP⁺;sox10⁺* OPCs within the white matter, and showing the rare occurance of OPCs located on the same side. (D-E) WT *Tg(olig2:egfp)* embryo with sox10 antibody labeling illustrating the position of which most OPCs are found. (G-I) *Tg(olig2:egfp)* embryo treated with HY at 24 hpf probed with *sox10* anitbody shows *EGFP⁻;sox10⁺* dorsally located OPCs and OPCs located within the grey matter. Scale bars represent 20 μm in all panels.

still dorsally positioned Sox 10^+/ EGFP$^-$ cells. The dorsal EGFP$^+$ cells are also very consistently located next to each other on the same side of the spinal cord. This may indicate two daughter cells arose from symmetric division of its progenitor when BMPs are inhibited.

Discussion

Could BMPs inhibit a different origin of oligodendrocytes?

In vitro work has used dorsal explants to provide evidence for a dorsal origin for oligodendrocytes that is inhibited by BMPs (Vallstedt et al., 2005). This work proposes a dorsal origin of oligodendrocytes exists but is prohibited from producing oligodendrocytes because of the high concentration of BMPs being secreted from the closely positioned roof plate. It is not until later in development when the concentration of BMPs is lower that this dorsal source can give rise to oligodendrocytes. This hypothesis has been very difficult to test in vivo because of the already existing oligodendrocytes that are migrating up from the pMN domain. Our data show a large increase in dorsally located Sox 10^+ OPCs by 48 hpf, an occurrence that rarely happens in a WT embryo. Usually when Sox 10^+ OPCs are present they colabel with EGFP, indicating that these cells migrated up from the pMN domain, arrived at their dorsal position and presumably begin to wrap axons making *mbp* to form myelin sheaths. The fact that these cells are Sox 10^+/EGFP$^-$ indicates that these OPCs did not migrate from the ventral EGFP expressing pMN domain. This may be the first in vivo evidence to support a

model of a dorsal origin of oligodendrocytes that is normally inhibited by secreted BMPs.

BMPs may be necessary for proper positioning of oligodendrocytes

As stated previously BMPs are secreted proteins and are critical for proper patterning within the spinal cord. The fact that OPCs seem to be improperly positioned within the grey matter rather than the white matter indicates that BMP signaling may be necessary for their migration into the white matter. However, HY is a very novel compound and we are not certain how long it can inhibit BMPs. It is possible within 2 days after treating embryos with the HY compound that the effects have worn off and a new wave of oligodendrocyte migration or differentiation has begun and these OPCs that are present within the grey matter have not reached their final destination. A closer look at the $EGFP^+$/Sox 10^+ cells within the grey matter would provide us with a better idea if this indeed the case.

CHAPTER V

CONCLUDING REMARKS

In this thesis we show that *olig2*, a bHLH transcription factor, identifies two distinct populations of *olig2*^{+} neurons located within the CNS. Efforts within the Appel lab have focused on *olig2*^{+} cells in the spinal cord, oligodendrocytes, the myelinating cell in the CNS (Lu et al., 2000; Park et al., 2002; Park et al., 2004). However, much of my work has focused on the patterning and formation of *olig2*^{+} cells within the zebrafish cerebellum, which we have identified as a distinct subset of PNs. My project has established DV organization between distinct subsets of PNs and eurydendroid neurons, and went on to determine Hh and Wnt signaling, morphogens with previously established roles for DV patterning within the spinal cord, play similar roles in patterning the DV axis of the zebrafish cerebellum (Ingham and McMahon, 2001; Jessell, 2000; Liem et al., 1997; Muroyama et al., 2002). My work has established Wnt signaling is necessary for the formation of *olig2*[+] PNs and suggests an antagonistic relationship between the ventral and dorsally located Shh and Wnt signals, although the mechanism by which this occurs is not exactly clear. I have also demonstrated how inhibition of BMP signaling, another signal known for its role in patterning the DV axis of the spinal cord, may influence specification of oligodendrocytes within the spinal cord. I have used transgenic lines, previously identified mutants, identified a novel cerebellar mutant, as well as utilized pharmacological agents to examine

loss of function and gain of function models to examine the role of these morphogens in formation, specification and patterning *olig2*^{+} cells throughout the CNS**.**

From a technical point of view, this work has brought forth some components that were previously hindering the ability to study the developing cerebellum, especially in zebrafish. Because of this work there are now multiple markers that we can use to identify several different cell types within the cerebellum. I have also developed a novel method of imaging the cerebellum to count cells within the cerebellum. Previous work has most often utilized sections for analysis, which does not allow for an analysis of its 3D structure, which was critical for this study.

From a scientific point of view, this work brings to light a role for Hh signaling that has been less explored. One common role Hh signaling is known for is promoting cell cycle exit. In mouse, zebrafish and flies, ectopic or overexpression of Hh signaling most often results in excessive proliferation. Some cancers, such as prostate cancer have been shown to have direct links to overactive Hh signaling resulting in tumor growth (Karhadkar et al., 2004; Sanchez et al., 2004; Sheng et al., 2004). The data presented in this thesis is much different in that when we block Hh signaling we see an increase in a population of PNs. My work exploring the roles of Hh and Wnt in *olig2*[+] PN development has shown that in contrast to the normal role for Hh, one role for Hh signaling in the developing *olig2*[+] PN population may be its ability to restrict Wnt signaling. Work in mouse and zebrafish have shown Wnt signaling has a critical

role in establishing the MBHB boundary, which is important for the actual formation of the cerebellum. This work has gone on to show that in the zebrafish cerebellum Wnt1 has an additional role. Loss of Wnt1 resulted in a loss of olig2+ and Zebrin II+ PNs. Suggesting for the first time Wnt1 is necessary for PN development.

REFERENCES

Alcedo, J., et al., 1996. The Drosophila smoothened gene encodes a seven-pass membrane protein, a putative receptor for the hedgehog signal. Cell. 86, 221-32.

Alder, J., et al., 1996. Embryonic precursor cells from the rhombic lip are specified to a cerebellar granule neuron identity. Neuron. 17, 389-99.

Alder, J., et al., 1999. Generation of cerebellar granule neurons in vivo by transplantation of BMP-treated neural progenitor cells. Nat Neurosci. 2, 535-40.

Alonso, J. R., et al., 1992. Parvalbumin immunoreactive neurons and fibres in the teleost cerebellum. Anat Embryol (Berl). 185, 355-61.

Altman, J., Bayer, S. A., 1978. Prenatal development of the cerebellar system in the rat. I. Cytogenesis and histogenesis of the deep nuclei and the cortex of the cerebellum. J Comp Neurol. 179, 23-48.

Altman, J., Bayer, S. A., 1984. The development of the rat spinal cord. Adv Anat Embryol Cell Biol. 85, 1-164.

Altman, J., Bayer, S. A., 1985. Embryonic development of the rat cerebellum. III. Regional differences in the time of origin, migration, and settling of Purkinje cells. J Comp Neurol. 231, 42-65.

Amit, S., et al., 2002. Axin-mediated CKI phosphorylation of beta-catenin at Ser 45: a molecular switch for the Wnt pathway. Genes Dev. 16, 1066-76.

Aruga, J., et al., 2002. Zic1 promotes the expansion of dorsal neural progenitors in spinal cord by inhibiting neuronal differentiation. Dev Biol. 244, 329-41.

Bally-Cuif, L., et al., 1995. Involvement of Wnt-1 in the formation of the mes/metencephalic boundary. Mech Dev. 53, 23-34.

Barresi, M. J., et al., 2000. The zebrafish slow-muscle-omitted gene product is required for Hedgehog signal transduction and the development of slow muscle identity. Development. 127, 2189-99.

Baurle, J., Grusser-Cornehls, U., 1997. Differential number of glycine- and GABA-immunopositive neurons and terminals in the deep cerebellar nuclei of normal and Purkinje cell degeneration mutant mice. J Comp Neurol. 382, 443-58.

Beachy, P. A., et al., 1997. Multiple roles of cholesterol in hedgehog protein biogenesis and signaling. Cold Spring Harb Symp Quant Biol. 62, 191-204.

Behrens, J., et al., 1996. Functional interaction of beta-catenin with the transcription factor LEF-1. Nature. 382, 638-42.

Belting, H. G., et al., 2001. spiel ohne grenzen/pou2 is required during establishment of the zebrafish midbrain-hindbrain boundary organizer. Development. 128, 4165-76.

Bhanot, P., et al., 1996. A new member of the frizzled family from Drosophila functions as a Wingless receptor. Nature. 382, 225-30.

Brand, M., et al., 1996. Mutations in zebrafish genes affecting the formation of the boundary between midbrain and hindbrain. Development. 123, 179-90.

Briscoe, J., Ericson, J., 2001. Specification of neuronal fates in the ventral neural tube. Curr Opin Neurobiol. 11, 43-9.

Briscoe, J., et al., 1999. Homeobox gene Nkx2.2 and specification of neuronal identity by graded Sonic hedgehog signalling. Nature. 398, 622-7.

Brochu, G., et al., 1990. Zebrin II: a polypeptide antigen expressed selectively by Purkinje cells reveals compartments in rat and fish cerebellum. J Comp Neurol. 291, 538-52.

Buckles, G. R., et al., 2004. Combinatorial Wnt control of zebrafish midbrain-hindbrain boundary formation. Mech Dev. 121, 437-47.

Cai, J., et al., 2005. Generation of oligodendrocyte precursor cells from mouse dorsal spinal cord independent of Nkx6 regulation and Shh signaling. Neuron. 45, 41-53.

Carstea, E. D., et al., 1997. Niemann-Pick C1 disease gene: homology to mediators of cholesterol homeostasis. Science. 277, 228-31.

Castro, A., et al., 2006. Calretinin immunoreactivity in the brain of the zebrafish, Danio rerio: distribution and comparison with some neuropeptides and neurotransmitter-synthesizing enzymes. I. Olfactory organ and forebrain. J Comp Neurol. 494, 435-59.

Celio, M. R., 1990. Calbindin D-28k and parvalbumin in the rat nervous system. Neuroscience. 35, 375-475.

Chang, A. C., Ghetti, B., 1993. Embryonic cerebellar graft development during acute phase of gliosis in the cerebellum of pcd mutant mice. Chin J Physiol. 36, 141-9.

Chen, D., et al., 2004. Bone morphogenetic proteins. Growth Factors. 22, 233-41.

Chen, J. K., et al., 2002. Inhibition of Hedgehog signaling by direct binding of cyclopamine to Smoothened. Genes Dev. 16, 2743-8.

Chen, W., et al., 2001. Analysis of the zebrafish smoothened mutant reveals conserved and divergent functions of hedgehog activity. Development. 128, 2385-96.

Chiang, C., et al., 1996. Cyclopia and defective axial patterning in mice lacking Sonic hedgehog gene function. Nature. 383, 407-13.

Christian, J. L., Nakayama, T., 1999. Can't get no SMADisfaction: Smad proteins as positive and negative regulators of TGF-beta family signals. Bioessays. 21, 382-90.

Christiansen, J. H., et al., 2000. Molecular control of neural crest formation, migration and differentiation. Curr Opin Cell Biol. 12, 719-24.

Clevers, H., van de Wetering, M., 1997. TCF/LEF factor earn their wings. Trends Genet. 13, 485-9.

Concordet, J. P., et al., 1996. Spatial regulation of a zebrafish patched homologue reflects the roles of sonic hedgehog and protein kinase A in neural tube and somite patterning. Development. 122, 2835-46.

Constam, D. B., Robertson, E. J., 1999. Regulation of bone morphogenetic protein activity by pro domains and proprotein convertases. J Cell Biol. 144, 139-49.

Cooper, M. K., et al., 1998. Teratogen-mediated inhibition of target tissue response to Shh signaling. Science. 280, 1603-7.

Crespo, C., et al., 1999. Distribution of parvalbumin immunoreactivity in the brain of the tench (Tinca tinca L., 1758). J Comp Neurol. 413, 549-71.

Currie, P. D., Ingham, P. W., 1996. Induction of a specific muscle cell type by a hedgehog-like protein in zebrafish. Nature. 382, 452-5.

Dahmane, N., Ruiz i Altaba, A., 1999. Sonic hedgehog regulates the growth and patterning of the cerebellum. Development. 126, 3089-100.

Davies, J. P., et al., 2000. Transmembrane molecular pump activity of Niemann-Pick C1 protein. Science. 290, 2295-8.

De Camilli, P., et al., 1984. Anatomy of cerebellar Purkinje cells in the rat determined by a specific immunohistochemical marker. Neuroscience. 11, 761-817.

de Zeeuw, C. I., Berrebi, A. S., 1996. Individual Purkinje cell axons terminate on both inhibitory and excitatory neurons in the cerebellar and vestibular nuclei. Ann N Y Acad Sci. 781, 607-10.

Diaz-Regueira, S., Anadon, R., 2000. Calretinin expression in specific neuronal systems in the brain of an advanced teleost, the grey mullet (Chelon labrosus). J Comp Neurol. 426, 81-105.

Dickinson, M. E., et al., 1995. Dorsalization of the neural tube by the non-neural ectoderm. Development. 121, 2099-106.

Dow, R. M., G 1958. The physiology and pathology of the cerebellum.

Echelard, Y., et al., 1993. Sonic hedgehog, a member of a family of putative signaling molecules, is implicated in the regulation of CNS polarity. Cell. 75, 1417-30.

Ekker, S. C., et al., 1995. Patterning activities of vertebrate hedgehog proteins in the developing eye and brain. Curr Biol. 5, 944-55.

Ericson, J., et al., 1997. Graded sonic hedgehog signaling and the specification of cell fate in the ventral neural tube. Cold Spring Harb Symp Quant Biol. 62, 451-66.

Ericson, J., et al., 1995. Sonic hedgehog: a common signal for ventral patterning along the rostrocaudal axis of the neural tube. Int J Dev Biol. 39, 809-16.

Fiez, J. A., 1996. Cerebellar contributions to cognition. Neuron. 16, 13-5.

Fine, E. J., et al., 2002. The history of the development of the cerebellar examination. Semin Neurol. 22, 375-84.

Friedland, N., et al., 2003. Structure of a cholesterol-binding protein deficient in Niemann-Pick type C2 disease. Proc Natl Acad Sci U S A. 100, 2512-7.

Futerman, A. H., van Meer, G., 2004. The cell biology of lysosomal storage disorders. Nat Rev Mol Cell Biol. 5, 554-65.

Geschwind, D. H., 1999. Focusing attention on cognitive impairment in spinocerebellar ataxia. Arch Neurol. 56, 20-2.

Gilthorpe, J. D., et al., 2002. The migration of cerebellar rhombic lip derivatives. Development. 129, 4719-28.

Goldowitz, D., Hamre, K., 1998. The cells and molecules that make a cerebellum. Trends Neurosci. 21, 375-82.

Gomes, W. A., et al., 2003. Transgenic overexpression of BMP4 increases astroglial and decreases oligodendroglial lineage commitment. Dev Biol. 255, 164-77.

Goodrich, L. V., et al., 1997. Altered neural cell fates and medulloblastoma in mouse patched mutants. Science. 277, 1109-13.

Grunwald, D. J., Eisen, J. S., 2002. Headwaters of the zebrafish -- emergence of a new model vertebrate. Nat Rev Genet. 3, 717-24.

Hager, G., et al., 1995. Novel forms of neuronal migration in the rat cerebellum. J Neurosci Res. 40, 207-19.

Hatten, M. E., Heintz, N., 1995. Mechanisms of neural patterning and specification in the developing cerebellum. Annu Rev Neurosci. 18, 385-408.

Hauptmann, G., Gerster, T., 2000. Multicolor whole-mount in situ hybridization. Methods Mol Biol. 137, 139-48.

Higashi, Y., et al., 1993. Cerebellar degeneration in the Niemann-Pick type C mouse. Acta Neuropathol (Berl). 85, 175-84.

Holmes, G., 1939. The Cerebellum of Man. Brain. 62, 30.

Huangfu, D., Anderson, K. V., 2006. Signaling from Smo to Ci/Gli: conservation and divergence of Hedgehog pathways from Drosophila to vertebrates. Development. 133, 3-14.

Ikenaga, T., et al., 2005. Morphology and immunohistochemistry of efferent neurons of the goldfish corpus cerebelli. J Comp Neurol. 487, 300-11.

Ikenaga, T., et al., 2006. Cerebellar efferent neurons in teleost fish. Cerebellum. 5, 268-74.

Ikeya, M., et al., 1997. Wnt signalling required for expansion of neural crest and CNS progenitors. Nature. 389, 966-70.

Imamura, T., et al., 1997. Smad6 inhibits signalling by the TGF-beta superfamily. Nature. 389, 622-6.

Ingham, P. W., McMahon, A. P., 2001. Hedgehog signaling in animal development: paradigms and principles. Genes Dev. 15, 3059-87.

Ito, M., 2000. Mechanisms of motor learning in the cerebellum. Brain Res. 886, 237-245.

Jessell, T. M., 2000. Neuronal specification in the spinal cord: inductive signals and transcriptional codes. Nat Rev Genet. 1, 20-9.

Karhadkar, S. S., et al., 2004. Hedgehog signalling in prostate regeneration, neoplasia and metastasis. Nature. 431, 707-12.

Karlstrom, R. O., et al., 2003. Genetic analysis of zebrafish gli1 and gli2 reveals divergent requirements for gli genes in vertebrate development. Development. 130, 1549-64.

Kawabata, M., Miyazono, K., 1999. Signal transduction of the TGF-beta superfamily by Smad proteins. J Biochem (Tokyo). 125, 9-16.

Kelly, G. M., Moon, R. T., 1995. Involvement of wnt1 and pax2 in the formation of the midbrain-hindbrain boundary in the zebrafish gastrula. Dev Genet. 17, 129-40.

Kenney, A. M., Rowitch, D. H., 2000. Sonic hedgehog promotes G(1) cyclin expression and sustained cell cycle progression in mammalian neuronal precursors. Mol Cell Biol. 20, 9055-67.

Kim, C. H., et al., 1997. Overexpression of neurogenin induces ectopic expression of HuC in zebrafish. Neurosci Lett. 239, 113-6.

Kimmel, C. B., et al., 1995. Stages of embryonic development of the zebrafish. Dev Dyn. 203, 253-310.

Kingsley, D. M., 1994. The TGF-beta superfamily: new members, new receptors, and new genetic tests of function in different organisms. Genes Dev. 8, 133-46.

Kishimoto, Y., et al., 1997. The molecular nature of zebrafish swirl: BMP2 function is essential during early dorsoventral patterning. Development. 124, 4457-66.

Ko, D. C., et al., 2005. Cell-autonomous death of cerebellar purkinje neurons with autophagy in Niemann-Pick type C disease. PLoS Genet. 1, 81-95.

Koster, R. W., Fraser, S. E., 2001. Direct imaging of in vivo neuronal migration in the developing cerebellum. Curr Biol. 11, 1858-63.

Krauss, S., et al., 1993. A functionally conserved homolog of the Drosophila segment polarity gene hh is expressed in tissues with polarizing activity in zebrafish embryos. Cell. 75, 1431-44.

Landis, S. C., Mullen, R. J., 1978. The development and degeneration of Purkinje cells in pcd mutant mice. J Comp Neurol. 177, 125-43.

Lannoo, M. J., et al., 1991a. Zebrin II immunoreactivity in the rat and in the weakly electric teleost Eigenmannia (gymnotiformes) reveals three modes of Purkinje cell development. J Comp Neurol. 310, 215-33.

Lannoo, M. J., Hawkes, R., 1997. A search for primitive Purkinje cells: zebrin II expression in sea lampreys (Petromyzon marinus). Neurosci Lett. 237, 53-5.

Lannoo, M. J., et al., 1991b. Development of the cerebellum and its extracerebellar Purkinje cell projection in teleost fishes as determined by zebrin II immunocytochemistry. Prog Neurobiol. 37, 329-63.

Lechtenberg, R. M. D., 1993. Handbook of Cerebellar Diseases. 573.

Lee, C. S., et al., 2001. Evidence that the WNT-inducible growth arrest-specific gene 1 encodes an antagonist of sonic hedgehog signaling in the somite. Proc Natl Acad Sci U S A. 98, 11347-52.

Lee, J., et al., 1997. Gli1 is a target of Sonic hedgehog that induces ventral neural tube development. Development. 124, 2537-52.

Lee, J. S., et al., 1999. Characterization of mouse dishevelled (Dvl) proteins in Wnt/Wingless signaling pathway. J Biol Chem. 274, 21464-70.

Lee, K. J., et al., 2000. Genetic ablation reveals that the roof plate is essential for dorsal interneuron specification. Nature. 403, 734-40.

Lee, K. J., Jessell, T. M., 1999. The specification of dorsal cell fates in the vertebrate central nervous system. Annu Rev Neurosci. 22, 261-94.

Lei, Q., et al., 2006. Wnt signaling inhibitors regulate the transcriptional response to morphogenetic Shh-Gli signaling in the neural tube. Dev Cell. 11, 325-37.

Lewis, K. E., Eisen, J. S., 2001. Hedgehog signaling is required for primary motoneuron induction in zebrafish. Development. 128, 3485-95.

Liem, K. F., Jr., et al., 2000. Regulation of the neural patterning activity of sonic hedgehog by secreted BMP inhibitors expressed by notochord and somites. Development. 127, 4855-66.

Liem, K. F., Jr., et al., 1997. A role for the roof plate and its resident TGFbeta-related proteins in neuronal patterning in the dorsal spinal cord. Cell. 91, 127-38.

Liem, K. F., Jr., et al., 1995. Dorsal differentiation of neural plate cells induced by BMP-mediated signals from epidermal ectoderm. Cell. 82, 969-79.

Lin, J. C., Cepko, C. L., 1998. Granule cell raphes and parasagittal domains of Purkinje cells: complementary patterns in the developing chick cerebellum. J Neurosci. 18, 9342-53.

Lin, J. C., Cepko, C. L., 1999. Biphasic dispersion of clones containing Purkinje cells and glia in the developing chick cerebellum. Dev Biol. 211, 177-97.

Liu, C., et al., 2002. Control of beta-catenin phosphorylation/degradation by a dual-kinase mechanism. Cell. 108, 837-47.

Liu, G., et al., 2003. A novel mechanism for Wnt activation of canonical signaling through the LRP6 receptor. Mol Cell Biol. 23, 5825-35.

Loftus, S. K., et al., 1997. Murine model of Niemann-Pick C disease: mutation in a cholesterol homeostasis gene. Science. 277, 232-5.

Logan, C. Y., Nusse, R., 2004. The Wnt signaling pathway in development and disease. Annu Rev Cell Dev Biol. 20, 781-810.

Lu, Q. R., et al., 2002. Common developmental requirement for Olig function indicates a motor neuron/oligodendrocyte connection. Cell. 109, 75-86.

Lu, Q. R., et al., 2000. Sonic hedgehog--regulated oligodendrocyte lineage genes encoding bHLH proteins in the mammalian central nervous system. Neuron. 25, 317-29.

Luiten, P. G., van der Pers, J. N., 1977. The connections of the trigeminal and facial motor nuclei in the brain of the carp (Cyprinus carpio L.) as revealed by anterograde and retrograde transport of horseradish peroxidase. J Comp Neurol. 174, 575-90.

Mann, R. K., Beachy, P. A., 2004. Novel lipid modifications of secreted protein signals. Annu Rev Biochem. 73, 891-923.

Marigo, V., Tabin, C. J., 1996. Regulation of patched by sonic hedgehog in the developing neural tube. Proc Natl Acad Sci U S A. 93, 9346-51.

Marti, E., et al., 1995. Requirement of 19K form of Sonic hedgehog for induction of distinct ventral cell types in CNS explants. Nature. 375, 322-5.

Marusich, M. F., et al., 1994. Hu neuronal proteins are expressed in proliferating neurogenic cells. J Neurobiol. 25, 143-55.

Mathis, L., et al., 1997. Retrospective clonal analysis of the cerebellum using genetic laacZ/lacZ mouse mosaics. Development. 124, 4089-104.

Mathis, L., Nicolas, J. F., 2003. Progressive restriction of cell fates in relation to neuroepithelial cell mingling in the mouse cerebellum. Dev Biol. 258, 20-31.

McMahon, A. P., Bradley, A., 1990. The Wnt-1 (int-1) proto-oncogene is required for development of a large region of the mouse brain. Cell. 62, 1073-85.

Meek, J., et al., 1992. Distribution of zebrin II in the gigantocerebellum of the mormyrid fish Gnathonemus petersii compared with other teleosts. J Comp Neurol. 316, 17-31.

Mekki-Dauriac, S., et al., 2002. Bone morphogenetic proteins negatively control oligodendrocyte precursor specification in the chick spinal cord. Development. 129, 5117-30.

Miller, J. R., Moon, R. T., 1997. Analysis of the signaling activities of localization mutants of beta-catenin during axis specification in Xenopus. J Cell Biol. 139, 229-43.

Miller, R. H., et al., 2004. Patterning of spinal cord oligodendrocyte development by dorsally derived BMP4. J Neurosci Res. 76, 9-19.

Miyawaki, S., et al., 1982. Sphingomyelinosis, a new mutation in the mouse: a model of Niemann-Pick disease in humans. J Hered. 73, 257-63.

Molven, A., et al., 1991. Genomic structure and restricted neural expression of the zebrafish wnt-1 (int-1) gene. Embo J. 10, 799-807.

Morales, D., Hatten, M. E., 2006. Molecular markers of neuronal progenitors in the embryonic cerebellar anlage. J Neurosci. 26, 12226-36.

Morton, S. M., Bastian, A. J., 2004. Cerebellar control of balance and locomotion. Neuroscientist. 10, 247-59.

Mueller, T., et al., 2006. A phylotypic stage in vertebrate brain development: GABA cell patterns in zebrafish compared with mouse. J Comp Neurol. 494, 620-34.

Mueller, T., Wullimann, M. F., 2003. Anatomy of neurogenesis in the early zebrafish brain. Brain Res Dev Brain Res. 140, 137-55.

Mullen, R. J., et al., 1976. Purkinje cell degeneration, a new neurological mutation in the mouse. Proc Natl Acad Sci U S A. 73, 208-12.

Munoz-Sanjuan, I., Brivanlou, A. H., 2002. Neural induction, the default model and embryonic stem cells. Nat Rev Neurosci. 3, 271-80.

Muroyama, Y., et al., 2002. Wnt signaling plays an essential role in neuronal specification of the dorsal spinal cord. Genes Dev. 16, 548-53.

Nakayama, T., et al., 2000. Regulation of BMP/Dpp signaling during embryonic development. Cell Mol Life Sci. 57, 943-56.

Niswander, L., Martin, G. R., 1993. FGF-4 regulates expression of Evx-1 in the developing mouse limb. Development. 119, 287-94.

Nusslein-Volhard, C., Wieschaus, E., 1980. Mutations affecting segment number and polarity in Drosophila. Nature. 287, 795-801.

Orentas, D. M., Miller, R. H., 1996. The origin of spinal cord oligodendrocytes is dependent on local influences from the notochord. Dev Biol. 177, 43-53.

Park, H. C., et al., 2002. olig2 is required for zebrafish primary motor neuron and oligodendrocyte development. Dev Biol. 248, 356-68.

Park, H. C., et al., 2004. Spatial and temporal regulation of ventral spinal cord precursor specification by Hedgehog signaling. Development. 131, 5959-69.

Parr, B. A., et al., 1993. Mouse Wnt genes exhibit discrete domains of expression in the early embryonic CNS and limb buds. Development. 119, 247-61.

Phillips, B. T., et al., 2006. Zebrafish msxB, msxC and msxE function together to refine the neural-nonneural border and regulate cranial placodes and neural crest development. Dev Biol. 294, 376-90.

Piccolo, S., et al., 1996. Dorsoventral patterning in Xenopus: inhibition of ventral signals by direct binding of chordin to BMP-4. Cell. 86, 589-98.

Pinson, K. I., et al., 2000. An LDL-receptor-related protein mediates Wnt signalling in mice. Nature. 407, 535-8.

Poh, A., et al., 2002. Patterning of the vertebrate ventral spinal cord. Int J Dev Biol. 46, 597-608.

Poncet, C., et al., 1996. Induction of oligodendrocyte progenitors in the trunk neural tube by ventralizing signals: effects of notochord and floor plate grafts, and of sonic hedgehog. Mech Dev. 60, 13-32.

Pringle, N. P., et al., 1996. Determination of neuroepithelial cell fate: induction of the oligodendrocyte lineage by ventral midline cells and sonic hedgehog. Dev Biol. 177, 30-42.

Ray, R. P., et al., 1991. The control of cell fate along the dorsal-ventral axis of the Drosophila embryo. Development. 113, 35-54.

Raymond, J. L., et al., 1996. The cerebellum: a neuronal learning machine? Science. 272, 1126-31.

Re'em-Kalma, Y., et al., 1995. Competition between noggin and bone morphogenetic protein 4 activities may regulate dorsalization during Xenopus development. Proc Natl Acad Sci U S A. 92, 12141-5.

Ribeiro, I., et al., 2001. Niemann-Pick type C disease: NPC1 mutations associated with severe and mild cellular cholesterol trafficking alterations. Hum Genet. 109, 24-32.

Riddle, R. D., et al., 1993. Sonic hedgehog mediates the polarizing activity of the ZPA. Cell. 75, 1401-16.

Rodriguez, F., et al., 2005. Cognitive and emotional functions of the teleost fish cerebellum. Brain Res Bull. 66, 365-70.

Roelink, H., Nusse, R., 1991. Expression of two members of the Wnt family during mouse development--restricted temporal and spatial patterns in the developing neural tube. Genes Dev. 5, 381-8.

Rotman, G., Shiloh, Y., 1997. Ataxia-telangiectasia: is ATM a sensor of oxidative damage and stress? Bioessays. 19, 911-7.

Roy, S., Ingham, P. W., 2002. Hedgehogs tryst with the cell cycle. J Cell Sci. 115, 4393-7.

Sanchez, P., et al., 2004. Inhibition of prostate cancer proliferation by interference with SONIC HEDGEHOG-GLI1 signaling. Proc Natl Acad Sci U S A. 101, 12561-6.

Schmidt, H., et al., 2007. Parvalbumin is freely mobile in axons, somata and nuclei of cerebellar Purkinje neurones. J Neurochem. 100, 727-35.

Schoenwolf, G. C., 1982. On the morphogenesis of the early rudiments of the developing central nervous system. Scan Electron Microsc. 289-308.

Schutter, D. J., van Honk, J., 2005. The cerebellum on the rise in human emotion. Cerebellum. 4, 290-4.

Schwaller, B., et al., 1993. Characterization of a polyclonal antiserum against the purified human recombinant calcium binding protein calretinin. Cell Calcium. 14, 639-48.

Semenov, M. V., et al., 2001. Head inducer Dickkopf-1 is a ligand for Wnt coreceptor LRP6. Curr Biol. 11, 951-61.

Sheng, T., et al., 2004. Activation of the hedgehog pathway in advanced prostate cancer. Mol Cancer. 3, 29.

Shin, J., et al., 2003. Neural cell fate analysis in zebrafish using olig2 BAC transgenics. Methods Cell Sci. 25, 7-14.

Shkumatava, A., Neumann, C. J., 2005. Shh directs cell-cycle exit by activating p57Kip2 in the zebrafish retina. EMBO Rep. 6, 563-9.

Solnica-Krezel, L., et al., 1994. Efficient recovery of ENU-induced mutations from the zebrafish germline. Genetics. 136, 1401-20.

Stoick-Cooper, C. L., et al., 2007. Distinct Wnt signaling pathways have opposing roles in appendage regeneration. Development. 134, 479-89.

Stolt, C. C., et al., 2002. Terminal differentiation of myelin-forming oligodendrocytes depends on the transcription factor Sox10. Genes Dev. 16, 165-70.

Strutt, D., 2003. Frizzled signalling and cell polarisation in Drosophila and vertebrates. Development. 130, 4501-13.

Taipale, J., Beachy, P. A., 2001. The Hedgehog and Wnt signalling pathways in cancer. Nature. 411, 349-54.

Taipale, J., et al., 2002. Patched acts catalytically to suppress the activity of Smoothened. Nature. 418, 892-7.

Takebayashi, H., et al., 2000. Dynamic expression of basic helix-loop-helix Olig family members: implication of Olig2 in neuron and oligodendrocyte differentiation and identification of a new member, Olig3. Mech Dev. 99, 143-8.

Tamai, K., et al., 2000. LDL-receptor-related proteins in Wnt signal transduction. Nature. 407, 530-5.

Tanabe, Y., Jessell, T. M., 1996. Diversity and pattern in the developing spinal cord. Science. 274, 1115-23.

Thach, W. T., et al., 1992. The cerebellum and the adaptive coordination of movement. Annu Rev Neurosci. 15, 403-42.

Thomas, K. R., Capecchi, M. R., 1990. Targeted disruption of the murine int-1 proto-oncogene resulting in severe abnormalities in midbrain and cerebellar development. Nature. 346, 847-50.

Tolwinski, N. S., et al., 2003. Wg/Wnt signal can be transmitted through arrow/LRP5,6 and Axin independently of Zw3/Gsk3beta activity. Dev Cell. 4, 407-18.

Tolwinski, N. S., Wieschaus, E., 2004. A nuclear escort for beta-catenin. Nat Cell Biol. 6, 579-80.

Traiffort, E., et al., 1998. Regional distribution of Sonic Hedgehog, patched, and smoothened mRNA in the adult rat brain. J Neurochem. 70, 1327-30.

Triarhou, L. C., 1998. Rate of neuronal fallout in a transsynaptic cerebellar model. Brain Res Bull. 47, 219-22.

Ulloa, F., et al., 2007. Inhibitory Gli3 activity negatively regulates Wnt/beta-catenin signaling. Curr Biol. 17, 545-50.

Urist, M. R., 1965. Bone: formation by autoinduction. Science. 150, 893-9.

Vallstedt, A., et al., 2005. Multiple dorsoventral origins of oligodendrocyte generation in the spinal cord and hindbrain. Neuron. 45, 55-67.

van de Wetering, M., et al., 1997. Armadillo coactivates transcription driven by the product of the Drosophila segment polarity gene dTCF. Cell. 88, 789-99.

van den Brink, G. R., et al., 2004. Indian Hedgehog is an antagonist of Wnt signaling in colonic epithelial cell differentiation. Nat Genet. 36, 277-82.

van Straaten, H. W., Hekking, J. W., 1991. Development of floor plate, neurons and axonal outgrowth pattern in the early spinal cord of the notochord-deficient chick embryo. Anat Embryol (Berl). 184, 55-63.

van Straaten, H. W., et al., 1985. Induction of an additional floor plate in the neural tube. Acta Morphol Neerl Scand. 23, 91-7.

Varga, Z. M., et al., 2001. Zebrafish smoothened functions in ventral neural tube specification and axon tract formation. Development. 128, 3497-509.

Wada, T., et al., 2000. Dorsal spinal cord inhibits oligodendrocyte development. Dev Biol. 227, 42-55.

Wall, N. A., Hogan, B. L., 1994. TGF-beta related genes in development. Curr Opin Genet Dev. 4, 517-22.

Wang, T., Morgan, J. I., 2007. The Purkinje cell degeneration (pcd) mouse: an unexpected molecular link between neuronal degeneration and regeneration. Brain Res. 1140, 26-40.

Wang, V. Y., Zoghbi, H. Y., 2001. Genetic regulation of cerebellar development. Nat Rev Neurosci. 2, 484-91.

Wassef, M., et al., 1986. Non-Purkinje cell GABAergic innervation of the deep cerebellar nuclei: a quantitative immunocytochemical study in C57BL and in Purkinje cell degeneration mutant mice. Brain Res. 399, 125-35.

Wechsler-Reya, R. J., Scott, M. P., 1999. Control of neuronal precursor proliferation in the cerebellum by Sonic Hedgehog. Neuron. 22, 103-14.

Wei, Q., et al., 2004. Sox10 acts as a tissue-specific transcription factor enhancing activation of the myelin basic protein gene promoter by p27Kip1 and Sp1. J Neurosci Res. 78, 796-802.

White, M., et al., 2000. Neuropsychologic and neuropsychiatric characteristics of patients with Friedreich's ataxia. Acta Neurol Scand. 102, 222-6.

Whitman, M., 1998. Smads and early developmental signaling by the TGFbeta superfamily. Genes Dev. 12, 2445-62.

Willert, K., et al., 2003. Wnt proteins are lipid-modified and can act as stem cell growth factors. Nature. 423, 448-52.

Wilson, L., Maden, M., 2005. The mechanisms of dorsoventral patterning in the vertebrate neural tube. Dev Biol. 282, 1-13.

Wine-Lee, L., et al., 2004. Signaling through BMP type 1 receptors is required for development of interneuron cell types in the dorsal spinal cord. Development. 131, 5393-403.

Wingate, R. J., 2001. The rhombic lip and early cerebellar development. Curr Opin Neurobiol. 11, 82-8.

Wingate, R. J., Hatten, M. E., 1999. The role of the rhombic lip in avian cerebellum development. Development. 126, 4395-404.

Wrana, J. L., et al., 1994. Mechanism of activation of the TGF-beta receptor. Nature. 370, 341-7.

Yamada, T., et al., 1991. Control of cell pattern in the developing nervous system: polarizing activity of the floor plate and notochord. Cell. 64, 635-47.

Yamashita, H., et al., 1996. Bone morphogenetic protein receptors. Bone. 19, 569-74.

Ye, W., et al., 1998. FGF and Shh signals control dopaminergic and serotonergic cell fate in the anterior neural plate. Cell. 93, 755-66.

Zhang, Y., Derynck, R., 1999. Regulation of Smad signalling by protein associations and signalling crosstalk. Trends Cell Biol. 9, 274-9.

Zhou, Q., Anderson, D. J., 2002. The bHLH transcription factors OLIG2 and OLIG1 couple neuronal and glial subtype specification. Cell. 109, 61-73.

Zhou, Q., et al., 2000. Identification of a novel family of oligodendrocyte lineage-specific basic helix-loop-helix transcription factors. Neuron. 25, 331-43.

Zhu, H., et al., 1999. A SMAD ubiquitin ligase targets the BMP pathway and affects embryonic pattern formation. Nature. 400, 687-93.

Zimmerman, L. B., et al., 1996. The Spemann organizer signal noggin binds and inactivates bone morphogenetic protein 4. Cell. 86, 599-606.